Review Article ISSN:2581-6284 Open Access

NANOTECHNOLOGY IN SCIENCE AND ENGINEERING

Journal Home Page: https://uniquepubinternational.com/upi-journals/nanotechnology-science-engineering-nse/

On the Nature of the Ion-Specific Effects

Stoyan I. Karakashev[1*], Nirav Raykundaliya[2]

[1]Department of Physical Chemistry, Sofia University, 1164 Sofia, Bulgaria.

[2]Marwadi Education Foundation, Rajkot, Gujarat, India.

Abstract

This article reports the effect of the counter-ions on the ionic surfactant adsorption layer and its relation to the stability of colloidal dispersions. The adsorption theory of Davies about the ionic surfactant monolayer is revisited and explored. Adsorption at the water|gas interface is compared to the water|oil interface, and the applicability of Langmuir's concepts for distributing pressure and liquid expanded film is shown. The detailed analysis clarifies the effects of the medium and the surfactant structure (hydrocarbon chain length, the nature of the container) on the adsorption. Extra accent is put on the Hofmeister effect of the counter-ion on the adsorption of ionic surfactants. The simple model of the van der Waals interaction of an ion with the interface was revisited, so taking into account the quantitative interpretation of the Hofmeister effect on the adsorption parameters. The core of this model stands a quantity called *ion specific adsorption energy* u_{i0}, which is related straightforwardly to basic ion characteristics, and is calculated for the counter-ions typically used in practice. An extended comparison with tensiometric and other experimental data demonstrates the usefulness of the theoretical models. The universality of the concept for the ion specific adsorption energy u_{i0} is further demonstrated by considering the role of the Hofmeister effect in two other phenomena, related to ionic surfactants: the disjoining pressure on thin liquid films and the stability of foams and emulsion. Unfortunately, the experimental data on the stability of foams and emulsions shows an opposite trend to our theoretical expectation – the stability increases upon the increase of the absolute value of the of the specific adsorption energy of the counter-ions in the water|gas or water|oil interfaces. It was shown abnormal effect of the

Funding Source(s): This work was supported by DT/IA Resource Centre, Ton Duc Thang University, Ho Chi Minh City, Vietnam.

Editorial History:
Received : 08-05-2018, Accepted: 12-07-2018,
Published: 13-07-2018

Correspondence to: Karakashev SI, Department of Physical Chemistry, Sofia University, 1164 Sofia, Bulgaria.
Email: fhsk@chem.uni-sofia.bg,
Telephone: +35928161283

How to Cite: Karakashev SI, Raykundaliya N. On the Nature of the Ion-Specific Effects. Nanotechnology in Science and Engineering 2018; 1(1): 21-60.

potassium counter-ion on the stability of foams. The later either act as a foamer or de-foamer depending on its concentration. To clarify the nature of this effect further investigations are required.

Key words: Ionic surfactants, Ion specific effects, Hofmeister series, Adsorption, Water|oil interface, Ion specific adsorption energy, Mixture of counter ions.

1. Introduction

The first works on the ion-specific effects were published by Hofmeister and coworkers more than 120 years ago. These works were focused on the solubility of blood proteins in presence of different salts [1-7]. Some salts were stronger precipitators than other ones. They ordered the cations and anions in order of their precipitation strength:

$$Li^+ < Na^+ < NH_4^+ < K^+ < Cs^+ < OH^- < F^- < CH_3COO^- < Cl^- < Br^- < NO_3^- < I^- < ClO_4^- \quad (1)$$

The ion sequence in the above series was found to be independent of the protein, although the effect depends on the sign of the protein's net charge as well. Since that time, many experimental studies showed similar dependencies in various phenomena. To explain the ion-specific effects, the ion size, the interaction of the ion with the water and the "hydration force" were the first factors taken into consideration [8]. Ninham and team [9] was the first to account for the van der Waals forces in the interaction between ions in solution, the adsorption of salts on hydrophobic surfaces, the interaction between proteins or colloidal particles etc. For example, they accounted for the van der Waals interaction between inorganic ions and the water|gas interface upon their adsorption [10-12]. At first their results were encouraging [12] but their further efforts to obtain good quantitative results met difficulties [13-15]. Tavares [16] studied theoretically the Hofmeister effect on the interaction of charged proteins. They calculated the purely electrostatic and the van der Waals contribution and found that the van der Waals interaction gives rise to a strong attractive force. In this work, we focus on the Hofmeister effect on the properties of adsorption layers of ionic surfactant on gas|water and oil|water interfaces and their relation to the stability of the dispersed systems.

Warszynski and team [17-19] clearly showed the specific effect of the counter-ions on the adsoprtion state of ionic surfactants. Aratono and team [20-22] conducted punctilious experiments coupled with thermodynamic analysis of the adsorption of a number of surfactants with various counter ions at gas|water and oil|water interfaces. It is worth to mention two theories, which did not address Hofmeister effect, but acted as a substabtial part in the theory of adsorption of ionic surfactants. The first one is the theory of Davies [23-24], who derived the important equation of state of dilute monolayers of ionic surfactants. The second theory belongs to Borwankar and Wasan [25] who proposed a simple approach for derivation of the adsorption isotherm of ionic surfactants.

Ivanov and team [26] followed the Ninham's approach, thus proposing and validating a relatively simple theory about the effect of the type of added electrolyte on the adsorption constant of the ionic surfactants. In the core of this theory is a quantity, u_{i0}, called *ion specific adsorption energy*, which is equal to the van der Waals

adsorption energy of an ion at the gas|water interface. It is a single, simple expression, accounting for all major factors controlling the ion specific adsorption: the ion polarizability and ionization potential, the radius of the hydrated ion and the possible deformation of the hydration shell upon ion adsorption at the interface. The ion specific adsorption energy u_{i0} turned out to be independent on the type of the surfactant, which allows one to combine theoretically the contributions from every type of counter-ion with all the possible surface active co-ions. In Ref. [27] the theory was successfully applied to disjoining pressure of thin liquid films, and emulsion stability. It was found out that the counter-ions with the smaller absolute value of the specific adsorption energy adsorb less on the film surfaces, thus rendering stronger electrostatic repulsion between the film surfaces. Accordingly, the counter-ions with larger absolute value of the specific adsorption energy adsorb more on the film surfaces, thus rendering weaker electrostatic repulsion between the film surfaces. Therefore, the first ones should stabilize the dispersions (foams and emulsions) more than the second ones. The experimental check on the stability of emulsions in presence of different counter-ions conducted in Ref. [27] showed the opposite dependence. To shed a light on this problem we investigated the stability of foams, stabilized by Sodium dodecylsulfate in presence of Li^+, Na^+, and K^+ counter-ions. Our investigation confirmed the trend reported by Ref.[27], bur revealed new scientific surprises.

2. Ion-Specific Effects on the Adsorption Layers of Ionic Surfactants from Dilute Solutions

2.1. Adsorption in the Absence of Ion Specific Effects

2.1.1. Henry's Adsorption Constant of Non-ionic Surfactants: Adsorption Energy and Thickness

We will start briefly with the basic theory about the scarce adsorption layer of the non-ionic surfactants. The chemical potentials of a non-ionic surfactant in an ideal solution of concentration C_s and in an ideal adsorbed monolayer of adsorption Γ_s are respectively:

$$\mu^B = \mu_0^B + k_B T \ln C_s, \quad (2)$$

$$\mu^S = \mu_0^S + k_B T \ln \Gamma_s. \quad (3)$$

Here superscripts "B" and "S" denote bulk and surface phase, and μ_0^S and μ_0^B are the corresponding standard chemical potentials. At equilibrium, the chemical potentials μ^B and μ^S must be equal. This leads to Henry's adsorption isotherm:

$$\Gamma_s = K_s C_s, \quad (4)$$

Where, the adsorption constant K_s is defined by the relation

$$k_B T \ln K_s \equiv \mu_0^B - \mu_0^S. \quad (5)$$

As it is obvious from the derivation, Henry's adsorption isotherm is valid only for adsorption layer consisting of non-interacting non-ionic surfactant molecules, which is possible for dilute adsorption layer only.

The first step in our analysis will be consideration of the dependence of K_s on the structure of the surfactant molecules and of the interface. The explicit expression for the adsorption constant K_s in terms of molecular parameters is usually written as:

$$K_s = \delta_a \exp(E_a / k_B T), \quad (6)$$

Where, δ_a is referred to as "thickness of the adsorbed layer", and E_a – as adsorption energy. Davies and Rideal (Equation 4.2 in Ref.[24]), proposed to use for the thickness δ_a the length of the surfactant molecule. Davies and Rideal represented the adsorption energy E_a as

$$E_a = E_0 + u_{CH_2} n_C. \quad (7)$$

Here n_C is the number of carbon atoms in the hydrophobic chain and u_{CH_2} is the (positive) free energy of transfer of a –CH_2– group from the solution into the adsorption layer. E_0 is the n_C-independent part of E_a which was ascribed in Refs. [28, 29] solely to the adsorption energy E_{head} of the hydrophilic head. In fact, both assumptions of Davies and Rideal for δ_a and E_a are not entirely correct.

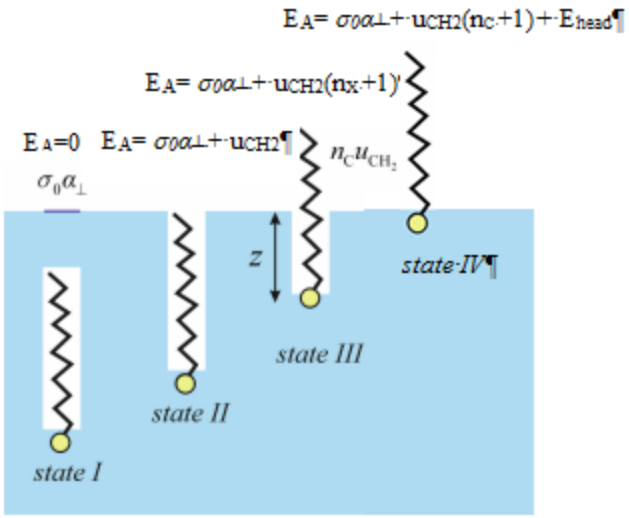

Figure 1. Four different stages from the adsorption of the surfactant molecule on gas|water interface: Stage I - Prior the very adsorption; Stage II - The cap of the hydrocarbon tail touches the gas|water interface; Stage III - Part of the hydrocarbon tail with n_x carbon atoms penetrated into the air's phase; Stage IV - The whole hydrocarbon tail with n_c carbon atoms penetrated into the air's phase.

(**i**) When the cap of the hydrophobic chain touches the surface, a portion of the water|hydrophobic phase interface, of area $\alpha_\perp$, disappears. The contribution of this process to $u(z)$ is modeled as a contact potential at $z = n_C l_{CH_2}$ (l_{CH_2} is length per –CH_2– group):

$$u_{(i)}(z) = \begin{cases} \sigma_0 \alpha_\perp, & z < n_C l_{CH_2}; \\ 0, & z > n_C l_{CH_2}, \end{cases} \quad (8)$$

Where σ_0 is the surface tension of the pure water|hydrophobic phase interface. For a typical oil, $\sigma_0 \approx 50 \times 10^{-3}$ J/m^2, so that energy $\sigma_0 \alpha_\perp$ is of the order of 10^{-20} J or about $2.5 \times k_B T$.

(**ii**) Let the free energy of transfer of a single –CH_2– group from the bulk solution to the adsorption layer be u_{CH_2}. For the energy u_{Me} of transfer of the –CH_3 group, we assume proportionality to the contact area of this group with water. One can approximate the shape of –CH_3 as a cylinder with a cap. The lateral area of the cylinder is assumed equal to that of a –CH_2– group, α_p, and the cap area is assumed equal to the cross-sectional area $\alpha_\perp$ of the hydrocarbon tail. The values of the two areas are $\alpha_\perp = \pi R_{CH_2}^2 \approx 21\ \text{Å}^2$ and $\alpha_p = 2\pi R_{CH_2} l_{CH_2} \approx 21\ \text{Å}^2$ (the values R_{CH_2} =2.6 Å for the cross-sectional radius of the chain and l_{CH_2} = 1.26 Å were used [30]. Consequently, the two areas are equal and the energy corresponding to each of these areas is $u_{CH_2}\alpha_p$. The energy pertaining to the cap can be represented as a contact potential with the same z-dependence as $u_{(i)}$ in Equation (8):

$$u_{(ii)}(z) = \begin{cases} u_{CH_2}, & z < n_C l_{CH_2}; \\ 0, & z > n_C l_{CH_2}. \end{cases} \tag{9}$$

The second part of u_{Me} (pertaining to the lateral area of –CH_3) is not included in Equation (9); it will be included in the next term, the potential $u_{(iii)}$.

(**iii**) Assuming for simplicity that the carbon chain remains normal to the interface, one can model the hydrophobic energy due to –CH_2– adsorption (plus the lateral energy of the –CH_3 group) as a linear function of the distance z between the surfactant head and the interface:

$$u_{(iii)}(z) = u_{CH_2} z / l_{CH_2}, \qquad n_C l_{CH_2} > z > 0. \tag{10}$$

(**iv**) Although the hydrophilic head remains immersed in the hydrophilic phase, it also interacts with the interface. This interaction probably involves both short-ranged and long-ranged (such as van der Waals and electrostatic) forces. Since these forces are not yet fully understood, we will account for their contribution to the adsorption energy E_a by an empirical constant E_{head}. Yet, the values of the adsorption energy of number of hydrophilic heads were determined and tabulated recently [31].

(**v**) One finally assumes that the surfactant cannot desorbs into the hydrophobic phase, i.e. $u(z) = \infty$ at $z < 0$.

Combining the contributions (**i**)-(**v**), one obtains an approximate expression for the interaction potential of a surfactant molecule with the interface (Figure 1):

$$u(z) = \begin{cases} \infty, & 0 > z; \\ -E_a + u_{CH_2} z / l_{CH_2}, & n_C l_{CH_2} > z > 0; \\ 0 & z > n_C l_{CH_2}, \end{cases} \tag{11}$$

Where the adsorption energy E_a is given by

$$E_a = E_{head} + \alpha_\perp \sigma_0 + u_{CH_2}\left(n_C + 1\right). \tag{12}$$

In Equation (11), the free energy of surfactant in the bulk solution is used as reference state. Comparison of Equations (12) and (7) leads to an explicit expression for the empirical constant E_0 of Davies and Rideal [24]:

$$E_0 = E_{\text{head}} + u_{\text{CH}_2} + \alpha_\perp \sigma_0 \tag{13}$$

It encompasses not only E_{head} as assumed by Davies and Rideal, but all the other contributions to E_a, unrelated to the adsorption of the –CH_2– chain. The last two terms are of the order of $1.4\times k_B T$ and $2.5\times k_B T$ correspondingly, while the experimental data give for E_{head} the order of several $k_B T$ [31].

Furthermore, we will show the derivation of the expression [29] for the "thickness of the adsorbed layer" δ_a, and the relation of δ_a and the adsorption energy E_a to the adsorption constant K_s. This can be done by statistical calculation of the adsorption Γ_s. Using Boltzmann distribution, the potential (11) and the Gibbs' definition of adsorption as an excess [32], for an ideal monolayer one can write:

$$\Gamma_s = C_s \int_0^{n_C l_{\text{CH}_2}} \left(e^{-u(z)/k_B T} - 1\right) dz = \frac{k_B T l_{\text{CH}_2}}{u_{\text{CH}_2}} e^{E_a/k_B T} \left(1 - e^{-n_C u_{\text{CH}_2}/k_B T} - \frac{n_C u_{\text{CH}_2}}{k_B T} e^{-E_a/k_B T}\right) C_s . \tag{14}$$

This is, in fact, a detailed expression of Henry's adsorption isotherm, $\Gamma_s = K_s C_s$. Since the exponents in the brackets are negligible, it yields the equation (6) for K_s. The comparison with Equation (6) shows that the adsorption layer thickness is

$$\delta_a = k_B T l_{\text{CH}_2} / u_{\text{CH}_2} . \tag{15}$$

Using Tanford's values for u_{CH_2} and l_{CH_2}, at 300°K, one obtains $\delta_a = 0.9$ and 1.2 Å for oil|water and W|G interfaces correspondingly. This is in contrast to the assumption that δ_a is of the order of the thickness of the adsorption layer [24]: indeed, for chain length $n_C = 12$, the ratio of the two thicknesses, $n_C l_{\text{CH}_2}$ and δ_a, as defined by Equation (15), is about 12.

2.1.2. Poisson-Boltzmann Equation and Electroneutrality (Gouy Equation)

Consider a solution of ionic surfactant in the presence or absence of added electrolyte positioned in the semi-space $z > 0$. Let each surfactant ion possess charge e_s (only monovalent surfactants will be considered, so that $e_s = \pm e_0$, where e_0 is the elementary charge). Consequently, the surface where the surfactants' heads are situated ($z = 0$) has a surface charge density $e_s\Gamma_s$, due to the surfactant adsorption in the adsorbed layer Γ_s. This surface charge and the ions in the diffuse layer create electrostatic potential $\phi(z)$ in the electrolyte solution, which is determined, in first approximation, by the Poisson-Boltzmann equation

$$\varepsilon \frac{d^2\phi}{dz^2} = -\sum_i e_i C_i \exp(-e_i\phi / k_B T) . \tag{16}$$

Here ε is the absolute dielectric constant, C_i and e_i are the i-th component bulk particle concentration and charge (in units [m^{-3}] and [C] correspondingly), k_B is the Boltzmann constant, T is absolute temperature. In this equation, the variables ϕ and $d\phi/dz \equiv -E$ (electric field) can be separated, by using the identity $2d^2\phi/dz^2 = d(E^2)/d\phi$. This leads to:

$$\mathrm{d}(E^2) = -\frac{2}{\varepsilon}\sum_i e_i C_i \exp(-e_i\phi / k_\mathrm{B}T)\mathrm{d}\phi\,. \tag{17}$$

A first integral of the Poisson-Boltzmann equation is obtained by integrating Equation (17) in limits $z = \infty$ to z, using as a first boundary condition $E = 0$ and $\phi = 0$ at $z = \infty$:

$$E(z)^2 = \frac{2k_\mathrm{B}T}{\varepsilon}\sum_i C_i\left(\mathrm{e}^{-e_i\phi(z)/k_\mathrm{B}T} - 1\right). \tag{18}$$

The second boundary condition (at $z = 0$) is the Gauss condition for electroneutrality:

$$\varepsilon E\big|_{z=0} = e_\mathrm{s}\Gamma_\mathrm{s}\,. \tag{19}$$

We will denote the surface potential $\phi(0)$ by ϕ^S. Setting $z = 0$ and $\phi = \phi^\mathrm{S}$ into Equation (18), and eliminating $E(z = 0)$ from the electroneutrality condition (19), the Gouy equation is obtained :

$$\frac{\kappa_0^2}{4}\Gamma_\mathrm{s}^2 = \sum_i C_i\left(\mathrm{e}^{-e_i\phi^\mathrm{S}/k_\mathrm{B}T} - 1\right). \tag{20}$$

Here

$$\kappa_0^2 \equiv 2e_0^2 / \varepsilon k_\mathrm{B}T \tag{21}$$

is the concentration independent part of Debye parameter: $\kappa^2 \equiv \kappa_0^2 C_\mathrm{t}$ and $\kappa_0^2 \equiv 2\times r_\mathrm{B}$, where $r_\mathrm{B} \equiv e_0^2 / \varepsilon k_\mathrm{B}T$ is the so-called Bjerumm length. In the case of 1:1 electrolyte, Gouy equation (20) simplifies to:

$$\frac{\kappa_0}{4}\Gamma_\mathrm{s} = \sqrt{C_\mathrm{t}}\sinh(\Phi^\mathrm{S}/2)\,. \tag{22}$$

Here C_t is the total electrolyte concentration (in units [m^{-3}]) and

$$\Phi^\mathrm{S} \equiv e_0\left|\phi^\mathrm{S}\right| / k_\mathrm{B}T \tag{23}$$

is the dimensionless positively defined surface potential. At high surface potentials ($\Phi^\mathrm{S} >> 1$), a good approximation of Gouy Equation (22) is

$$\Gamma_\mathrm{s} = \frac{2}{\kappa_0}\sqrt{C_\mathrm{t}}\exp(\Phi^\mathrm{S}/2)\,. \tag{24}$$

In the case of 1:1 electrolyte, Equation (18) can be integrated analytically. First, we take the root of Equation:

$$\frac{\mathrm{d}e_0\phi(z)/k_\mathrm{B}T}{\mathrm{d}z} = -\kappa_0\sqrt{C_\mathrm{t}}\left(\mathrm{e}^{e_0\phi(z)/2k_\mathrm{B}T} - \mathrm{e}^{-e_0\phi(z)/2k_\mathrm{B}T}\right). \tag{25}$$

Direct integration of Equation (25) gives an explicit relation between z and ϕ:

$$\kappa_0\sqrt{C_\mathrm{t}}\,z/2 = \operatorname{arctanh}\left(\mathrm{e}^{e_0\phi/2k_\mathrm{B}T}\right) - \operatorname{arctanh}\left(\mathrm{e}^{e_0\phi^\mathrm{S}/2k_\mathrm{B}T}\right). \tag{26}$$

2.1.3. Thermodynamics of the Diffuse Double Layer: Adsorption and Surface Tension

The ion distribution in the electrical double layer depends on the local potential $\phi(z)$. The ion adsorption Γ_j^DL of any ion *j in the diffuse layer* can be calculated by using Gibbs' definition of adsorption as an excess:

$$\Gamma_j^{\mathrm{DL}} \equiv C_j \int_0^{\infty} \left(\mathrm{e}^{-e_j \phi(z)/k_{\mathrm{B}}T} - 1 \right) \mathrm{d}z \,, \tag{27}$$

Where, the superscript "DL" indicates adsorption of the counter-ions, co-ions and surfactant ions in the double layer only. In principle, the *total* surfactant adsorption is a sum of $\Gamma_{\mathrm{s}}^{\mathrm{DL}}$ and the surface concentration Γ_{s} (which is the adsorption in the adsorption layer, driven by hydrophobic forces). The surfactant ions in the diffuse layer are repelled by the interface since they have the same charge. Usually, the surface potential Φ^{S} is high, so that the surfactant concentration in the diffuse layer is close to zero. This leads to a relatively small negative absorption of the order of $\Gamma_{\mathrm{s}}^{\mathrm{DL}} \sim -C_{\mathrm{s}}/\kappa$. Since $|\Gamma_{\mathrm{s}}^{\mathrm{DL}}| << \Gamma_{\mathrm{s}}$, the adsorption of surfactant in the diffuse layer can be neglected. The same refers to the co-ions. Hence, under these conditions only the adsorption of the counter-ions in the diffuse layer is of importance.

In order to calculate the integrals defined by Equation (27), it is convenient to change the integration variable to ϕ, by using the relation $\mathrm{d}z = \mathrm{d}\phi / \left(\mathrm{d}\phi / \mathrm{d}z \right)$,

$$\Gamma_j^{\mathrm{DL}} \equiv C_j \int_{\phi^{\mathrm{S}}}^{0} \frac{\exp(-e_j \phi / k_{\mathrm{B}}T) - 1}{\mathrm{d}\phi / \mathrm{d}z} \mathrm{d}\phi \,. \tag{28}$$

By inserting here the expression (25) for $\mathrm{d}\phi/\mathrm{d}z$, one can obtain explicit formulae for the adsorptions Γ_j^{DL}. For 1:1 electrolyte at high surface potential Φ^{S}, the result for the adsorption of the counterion i reads

$$\Gamma_i^{\mathrm{DL}} = \frac{2C_i}{\kappa_0 \sqrt{C_{\mathrm{t}}}} \left(\mathrm{e}^{\Phi^{\mathrm{S}}/2} - 1 \right) \xrightarrow{\Phi^{\mathrm{S}} \to \infty} \frac{2C_i}{\kappa_0 \sqrt{C_{\mathrm{t}}}} \exp(\Phi^{\mathrm{S}}/2) \,. \tag{29}$$

To calculate the surface tension, the Gibbs isotherm is used. If only one counter-ion of concentration C_i is present in the system, and the bulk solution is assumed ideal, one has

$$\mathrm{d}\sigma = -k_{\mathrm{B}}T\Gamma_{\mathrm{s}} \mathrm{d}\ln C_{\mathrm{s}} - k_{\mathrm{B}}T\Gamma_i^{\mathrm{DL}} \mathrm{d}\ln C_i \,. \tag{30}$$

Since at high surface potential the charge of the adsorbed layer is compensated only by the counter-ion in the diffuse layer, one has $\Gamma_i^{\mathrm{DL}} = \Gamma_{\mathrm{s}}$. Then, the Gibbs isotherm (30) simplifies to

$$\mathrm{d}\sigma = -2k_{\mathrm{B}}T\Gamma_{\mathrm{s}} \mathrm{d}\ln C \,, \tag{31}$$

where C is the mean ionic activity of the surfactant [33, 34], defined by:

$$C = C_{\mathrm{s}}^{1/2} C_i^{1/2} \,. \tag{32}$$

If the solution is not ideal, the mean ionic activity C in Equation (31) will include activity coefficient γ:

$$C = \gamma C_{\mathrm{s}}^{1/2} C_i^{1/2} \,. \tag{33}$$

2.1.4. Davies Adsorption Isotherm

We now consider an ideal solution of ionic surfactant of concentration C_{s} in equilibrium with an "ideal" charged adsorbed monolayer with surface potential ϕ^{S}. The chemical potentials in the two states are

$$\mu^{\mathrm{B}} = \mu_0^{\mathrm{B}} + k_{\mathrm{B}}T \ln C_{\mathrm{s}}; \qquad \mu^{\mathrm{S}} = \mu_0^{\mathrm{S}} + k_{\mathrm{B}}T \ln \Gamma_{\mathrm{s}} + e_{\mathrm{s}}\phi^{\mathrm{S}}. \tag{34}$$

The difference with the corresponding expressions for nonionic surfactants, Equations (2)-(3), is the presence of the additional electrostatic energy term $e_s\phi^S$ in μ^S.

The condition for equilibrium between the surfactant molecules in the bulk solution and at the surface reads:

$$\mu_0^{\mathrm{B}} + k_{\mathrm{B}}T \ln C_{\mathrm{s}} = \mu_0^{\mathrm{S}} + k_{\mathrm{B}}T \ln \Gamma_{\mathrm{s}} + e_{\mathrm{s}}\phi^{\mathrm{S}}. \tag{35}$$

Introducing here the dimensionless potential Φ^S, Equation (23), one obtains

$$\Gamma_{\mathrm{s}} = K_{\mathrm{s}}C_{\mathrm{s}} \exp(-\Phi^{\mathrm{S}}). \tag{36}$$

Equation (36) was first derived by Davies [23, 24]; see also Ref. [25]. The adsorption constant K_s in this equation is defined by Equation (5), but in this case $\mu_0^B - \mu_0^S$ may contain electrostatic contributions.

The elimination of Γ_s from Equations (24) and (36) leads to an equation for the dependence of the surface potential Φ^S on the composition of the bulk solution [23, 29]:

$$3\Phi^{\mathrm{S}} = \ln \frac{\kappa_0^2 K_{\mathrm{s}}^2}{4} + \ln \frac{C_{\mathrm{s}}^2}{C_{\mathrm{t}}} = 6 \ln \frac{\kappa_0 K_0}{2} + \ln \frac{C_{\mathrm{s}}^2}{C_{\mathrm{t}}}. \tag{37}$$

Equation (37) shows that the surface potential Φ^S increases with C_s and K_s (due to the increased adsorption) and decreases with the total electrolyte concentration C_t (due to the additional screening effect of the electrolyte on the surface charge).

Inserting back the surface potential (37) into the isotherm (36), one obtains a generalization of Henry's isotherm for adsorption of ionic surfactants:

$$\Gamma_{\mathrm{s}} = K_0 C^{2/3}, \tag{38}$$

where C is given by Equation (32), and K_0 is adsorption constant of the ionic surfactant. It is related to Henry's constant K_s:

$$K_0 = \left(4K_{\mathrm{s}} / \kappa_0^2\right)^{1/3}. \tag{39}$$

The fact that according to Equation (38) Γ_s depends only on the mean ionic activity C is an explicit formulation of what is known as *salting out effect* on ionic surfactant adsorption [34]. Equation (38) was first derived and confirmed by experimental data for $C_nH_{2n+1}SO_4^+$ at W|G interface by Davies [23]. We will refer to it as Davies isotherm. By using the procedure of Borwankar and Wasan [25], and Ivanov team derived Equation (38) and obtained the explicit expression (39) for K_0. According to Equation (39), K_0 should not depend on the electrolyte concentration, at least for moderate concentrations.

Substituting Equation (38) in the Gibbs isotherm (31) and integrating, one obtains the surface pressure isotherm:

$$\pi^{\mathrm{S}} \equiv \sigma_0 - \sigma = 3k_{\mathrm{B}}TK_0C^{2/3}, \tag{40}$$

which is due also to Davies [35]. Comparison with Equation (38) shows that $\pi^{S} = 3k_{B}T\Gamma_{s}$. Since the surface pressure of an ideal layer of a nonionic surfactant is $k_{B}T\Gamma_{s}$, it follows that the contribution to π^{S} of the double layer at high surface potential is

$$\pi_{el}^{S} = 2k_{B}T\Gamma_{s}. \quad (41)$$

For the sake of simplicity, until now the ever present counter-ion specific effects were disregarded. It will be shown in Section 0, that these effects modify the adsorption constant, leading instead of K_0 in Equations (38) and (40) to a new constant, $K = K_0\exp(-u_{i0}/2k_{B}T)$, where u_{i0} is the counter-ion specific adsorption energy (cf. Equation (55) below).

2.2. Adsorption Behavior at Water|Gas Versus Oil|Water Interface: Liquid Expanded Layer and Spreading Pressure

We analyze below the experimental data for π^{S} vs. the 2/3-power of the mean ionic activity $C^{2/3}$ at oil|water and air|water for low and medium surfactant concentrations – data for sodium dodecylsulfate, $C_{12}H_{25}SO_4Na$, at oil|water and air|water in the presence of various concentrations of $NaCl$ are shown in Figure 1. At air|water, the data exhibit two well defined regions. At very low surface pressures (less than ca. 2-3 mN/m), a close-to-linear dependence without intercept is observed. At intermediate concentrations (up to CMC) and pressures, there is a second linear region, but with negative intercept. Denoting this intercept by π_0, one can write for this region instead of Equation (40):

$$\pi^{S} = \pi_0 + 3k_{B}TK^{LE}C^{2/3}. \quad (42)$$

By analogy with Langmuir's treatment of non-charged monolayers [36], this behavior can be explained by assuming that the monolayer is in liquid expanded (LE) state. In this state the adsorbed hydrophobic tails form a very thin, but more or less dense oil film spread onto the water phase. In contrast, in the first region, at lower concentrations, the surfactant molecules are in gaseous state, where they are isolated from each other. The intersection point between the two lines probably corresponds to phase transition between the gaseous and the LE states (Figure 1). Langmuir's idea for the origin of π_0 (e.g.[36]) can be quantified as follows. Let σ_0^{WO} be the interfacial tension of the pure oil|water interface, and σ_0^{OG} be the air|water surface tension. The oil-like thin film formed by the adsorbed hydrophobic tails can be considered as a single "interface" (membrane) of interfacial tension $\sigma_0^{M} = \sigma_0^{WO} + \sigma_0^{OG}$, which for this system is the counterpart of the interfacial tension of the pure interface σ_0. The hydrophilic heads of the surfactant are "adsorbed" at the water|oil interface of the thin film. If their adsorption is ideal one can use Equation (40) with σ_0 replaced with σ_0^{M} to calculate σ:

$$\sigma = \sigma_0^{OG} + \sigma_0^{WO} - 3k_{B}TK^{LE}C^{2/3}. \quad (43)$$

However, by definition, the surface pressure π^S at W|G is defined with respect to the clean W|G surface of tension σ_0^{WG}, that is, $\pi^S = \sigma_0^{WG} - \sigma$. Inserting Equation (43) into this definition, and comparing the result to Equation (42), one obtains

$$\pi_0 = \sigma_0^{WG} - \sigma_0^{WO} - \sigma_0^{OG}. \quad (44)$$

According to these simple considerations, the intercept π_0 coincides with the spreading coefficient of a hydrocarbon on water [29]. Therefore, π_0 is referred to as *spreading pressure*. Langmuir's explanation of π_0 is confirmed by the data in Figure 1. Indeed, the spreading coefficient of dodecane on water is –6.4 mN/m (the values $\sigma_0^{WO} = 53.7$, $\sigma_0^{OG} = 25.3$ and $\sigma_0^{WG} = 72.6$ mN/m at 22°C were used, vs. $\pi_0 = -7$ mN/m determined from the data in Figure 1. However, this picture is oversimplified, and as will be shown in Section 0 below, π_0, in fact, depends on the counterion (cf. Figure 10), and probably – on the surfactant ionic head. The reason for these dependences is not yet clear.

The situation is different with the adsorption at the oil|water. In this case, there is no interface oil|gas. Then, one must replace in Equation (44) σ_0^{WG} by σ_0^{WO}, and σ_0^{OG} by σ_0^{OO} (the latter is of course zero). Thus one finds $\pi_0 = 0$, in accordance with the data in Figure 1: indeed, the surface pressure at oil|water follows rather well the simple dependence (40) with no intercept, up to $C^{2/3} \approx 2$ mM$^{2/3}$ ($C \approx 3$ mM).

The following observations deserve additional attention:

(**i**) In accordance with the salting out effect and Equation (31), the surface tension σ depends on the mean activity C only, as defined by Equation (33). Indeed, regardless of the electrolyte concentrations, all data fall on 2 master-curves π^S vs. $C^{2/3}$ (one for air|water and one for alkane|water). This is so only if activities rather than concentrations are used – this follows also from Equation (31). The activity coefficients γ in Figure 1 were calculated by the formula [33].

$$\lg \gamma = -\frac{A\sqrt{C_t}}{1 + B\sqrt{C_t}} + bC_t. \quad (45)$$

If the total electrolyte concentration $C_t = C_{el} + C_s$ is in units [M], the Debye constant is $A = 0.5108$ M$^{-1/2}$ (at 298.15 K); for the empirical constants B and b we used the mean values $B = 1.25$ M$^{-1/2}$ and $b = 0.0083$ M^{-1} for all salts.

(**ii**) The dependence of π^S on $C^{2/3}$ is linear up to surface pressures of about 25 mN/m for W|O and 30 mN/m for air|water (the values of the slopes and the adsorption parameters are listed in Table 1). The respective values of $C^{2/3}$ are about 1.8 mM$^{2/3}$ and 3.2 mM$^{2/3}$. The difference between the two systems is due to the larger second virial coefficient (larger repulsive interactions) at the oil|water, which leads to earlier deviation from ideality. This is evident from the values of the respective second virial coefficients.

(**iii**) At air|water the line drawn for the gaseous adsorbed layer is tentative only, as far as the validity of Davies isotherm in this region is questionable due to the low potential and the possible effects of the charge

discreteness. Phase transition from gaseous to LE state occurs at the air|water at $C = 0.81$ mM, corresponding to π^S about 3.0 mN/m found 0.83 mM and 3.9 mN/m respectively). This corresponds to transition from $\Gamma_s = 0.24$ nm^{-2} to $\Gamma_s = 0.78$ nm^{-2}, i.e. from less dense gaseous structure to a more dense liquid-like monolayer (see the $\Gamma_s(C^{2/3})$ plot in Figure 1).

(**iv**) A number of different procedures were tested to determine K, including linear regression on few initial points (straight lines in Figure 1) and square polynomial fit (long dashed curve in Figure 1) with the equation

$$\pi^S = \pi_0 + 3k_BTKC^{2/3} + bC^{4/3}, \quad (46)$$

Although the linear regression model looks satisfactory, we preferred the result from the polynomial fit because it generally yields K values closer to the ones obtained by using more realistic models.

(**v**) From the $\pi^S(C^{2/3})$ data and Equation (46), we found for the LE region $K^{LE} = 156$ (cf. Table 1). The latter is very close to the value for adsorption at air|water, $K^{WO} = 178$, which suggests that both processes are similar.

Davies also accounted for the cohesive (i.e., negative spreading) pressure of soluble ionic surfactants at the air|water [23, 24]. However, neither Langmuir [36]] nor Davies [23] used the simple isotherm (43). Instead, Langmuir used a correction for steric repulsion between the heads, while Davies introduced an empirical dependence of π_0 on Γ_s.

In Figure 2, the Davies model was tested further by comparison of the theoretical surface potential ϕ^S, cf. Equation (37), with ζ-potential measurements of the water|hexadecane interface. All parameters in Equation (37) are known. In fact, the experimental data involve also ion specific effects. Hence, the calculation of ϕ^S was performed with Equations (55) and (57), whith account for the effect of the counterion of K and on ϕ^S; the value $u_{i0} = -0.34\ k_BT$ was used for Na^+, cf. Table 2. It turned out that the contribution of the ion specific effect is small.

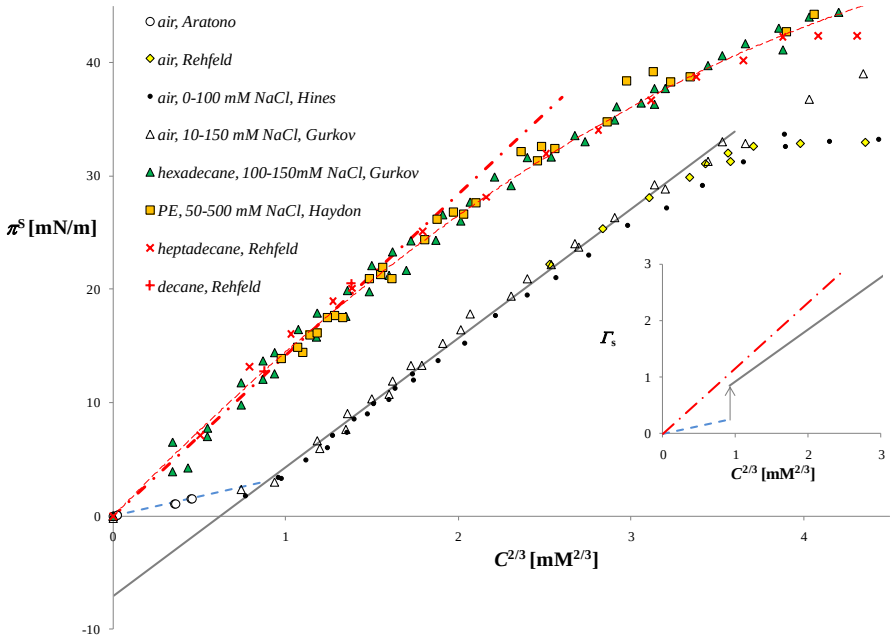

Figure 1. Interfacial pressure π^S vs. the 2/3-power of the mean activity $C^{2/3}$ for $C_{12}H_{25}SO_4Na$ solutions at different $NaCl$ concentrations. Data for air|water [37-40] and oil|water; oil is heptadecane, decane [39], hexadecane [38], petroleum ether [41]. Solid line: fit of data for the W|G in the range $C^{2/3} = 1.2 \div 3$ $mM^{2/3}$ (the LE region), according to Equation (42). The short dash line stands for water|gas data in the range $C^{2/3} = 0 \div 1$ $mM^{2/3}$ (gaseous monolayer region). Dash-dot line: fit of air|water data in the range $C^{2/3} = 0 \div 1.8$ $mM^{2/3}$, Equation (40). Long dash line: quadratic fit of oil|water data in the range $C^{2/3} = 0 \div CMC^{2/3}$, Equation (46). The adsorption parameters determined from these fits are listed in Table 1. In the inset: the corresponding adsorption isotherms, $\Gamma_s(C^{2/3})$, calculated from Equation (38) with the adsorption parameters determined by the fits. The jump of Γ_s at $C = 0.81$ mM corresponds to a phase transition from gaseous monolayer to LE state.

Table 1. Values of the adsorption parameters, determined from the data in Figure 1, according to Equation (46) for W|O and Equation (42) for air|water (T = 25°C).

Parameter	linear Fit with Equation (42)			Quadratic Fit (46)	
	$d\pi^S/dC^{2/3}$ [mN/mM$^{2/3}$m]	π_0 [mN/m]	K	π_0 [mN/m]	K
W|G, LE	11.4	–7.0	129	-9.1	156
W|O	13.5	0	161	0	178

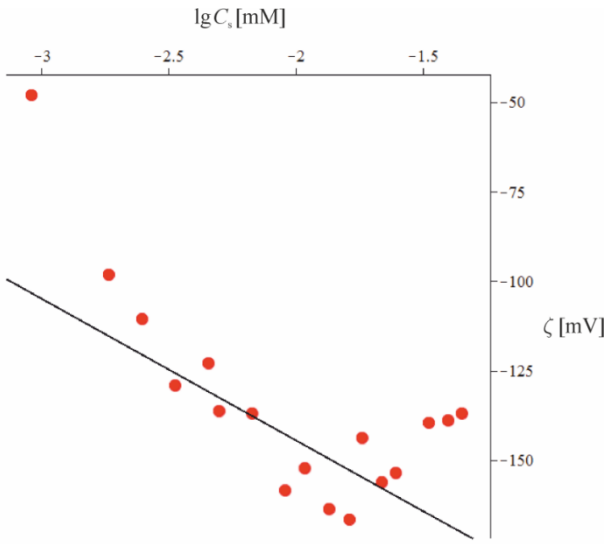

Figure 2. Dependence of the ζ-potential [mV] at hexadecane|water interface on $\lg C_s$ [mM] (C_s is concentration of $C_{12}H_{25}SO_4^-Na^+$), in the presence of 10 mM NaCl [38]. Solid line: theoretical dependence, Equation (37), of the surface potential ϕ^S (assumed equal to the ζ-potential) on C_s, with no adjustable parameters ($K = 178$, Table 1).

2.3. Counterion Specific Effects on the Adsorption of Ionic Surfactants from Diluted Solutions

2.3.1. Gouy Equation with Specific Interactions

We turn now to the theoretical treatment of the influence of the van der Waals interactions (which we consider as the most important specific interaction) of the counter-ions with the interface on the adsorption of a monovalent ionic surfactant. Toward this goal an extended Poisson-Boltzmann equation, involving both electrostatic and van der Waals potentials, is solved approximately. The ensuing generalized form of Gouy equation, along with some thermodynamic considerations, will be used in the remaining parts of this Chapter to account for the ion specific effects on the adsorption and related phenomena with ionic surfactants.

Near the adsorbed layer of an ionic surfactant, the van der Waals forces between the counter-ion and the bulk phases lead to an increase of the counter-ion local concentration in the diffuse double layer. The repulsive interactions disallow the counter-ion to approach the interface at distance smaller than its radius *R* (bare or hydrated). Both interactions, repulsive and attractive, were modeled in a simple manner in Refs. [26, 29] by the following expression for the energy $u_i(z)$ of specific interaction between the ion and the interface:

$$u_i(z) = \frac{R_i^3}{\left(R_i + z\right)^3} u_{i0} \,. \tag{47}$$

Here R_i is the ionic radius and u_{i0} is the van der Waals energy of an ion in the plane $z = 0$ situated at distance R_i from the interface (Figure 3). If one assumes that the van der Waals energy (47) and the electrostatic energy $e_i\phi^S$ are additive, the Boltzmann distribution will involve the sum of the two: $e_i\phi^S + u_i(z)$. The Poisson-Boltzmann equation (16) will then read:

$$\varepsilon \frac{\mathrm{d}^2\phi}{\mathrm{d}z^2} = -\sum_i e_i C_i \, \mathrm{e}^{-(e_i\phi + u_i(z))/k_\mathrm{B}T} \,. \tag{48}$$

This equation can be integrated by analogy with the derivation of Gouy equation (20), by using $2\mathrm{d}^2\phi/\mathrm{d}z^2 = \mathrm{d}(E^2)/\mathrm{d}\phi$ and the Gauss condition (19) The result is:

$$e_0^2 \Gamma_\mathrm{s}^2 = -2\varepsilon \sum_i e_i C_i \, \mathrm{e}^{-u_{i0}/k_\mathrm{B}T} \int_0^{\phi^S} \mathrm{e}^{-e_i\phi/k_\mathrm{B}T} \, \mathrm{e}^{-(u_i(z)-u_{i0})/k_\mathrm{B}T} \, \mathrm{d}\phi \,. \tag{49}$$

At high surface potentials, only the counter-ions need to be taken into account in the sum in the right-hand side of this equation. This approximation is of crucial importance for the success of our theory for it simplifies all following calculations. It can be used also in the case of ionized proteins and polymers (when $|\phi^S/k_\mathrm{B}T| >> 1$), but not for the adsorption of simple electrolytes. In the latter case, both cations and anions (whose properties are similar) have comparable participation in the diffuse layer whose local potential depends, in fact, on the small difference of their local concentrations. With this approximation, the integrals in the right hand side of Equation (49) can be evaluated by using an iterative procedure [26]. As zeroth iteration, one can use in the integrand the results for the case of absent ion specific effect by setting it in Equation (49) $\phi^S = \phi_0^S$, where ϕ_0^S is given by Equation (37), and $z = z_0(\phi)$,, given by Equation (26). Integration by parts then leads to

$$\int_0^{\phi_0^S} \mathrm{e}^{-e_i\phi/k_\mathrm{B}T} \, \mathrm{e}^{-(u_i(z_0)-u_{i0})/k_\mathrm{B}T} \, \mathrm{d}\phi = -\frac{k_\mathrm{B}T}{e_i} \mathrm{e}^{\phi_0^S} \left(1 - F_u\right), \tag{50}$$

Where F_u stands for the expression

$$F_u = \mathrm{e}^{-\Phi_0^{\mathrm{S}}}\left[\mathrm{e}^{u_{i0}/k_{\mathrm{B}}T} + \int_0^{\phi_0^{\mathrm{S}}} \mathrm{e}^{-e_i\phi/k_{\mathrm{B}}T}\,\frac{\mathrm{d}\,\mathrm{e}^{-(u_i(z_0)-u_{i0})/k_{\mathrm{B}}T}}{\mathrm{d}\phi}\,\mathrm{d}\phi\right]. \tag{51}$$

At high surface potentials, the value of F_u was found much smaller than unity [26], so that it can be neglected in Equation (50). Using this approximation, one substitutes Equation (50) into Equation (49) to obtain a generalization of Gouy equation (20), accounting for the ion specific effect:

$$\Gamma_{\mathrm{s}}^2 = \frac{4}{\kappa_0^2}\sum_i C_i\,\mathrm{e}^{-u_{i0}/k_{\mathrm{B}}T}\,\mathrm{e}^{\Phi_0^{\mathrm{S}}} \tag{52}$$

(The Debye parameter κ_0 is given by Equation (21)). If only one counterion is present in the system, Equation (52) simplifies to

$$\Gamma_{\mathrm{s}}^2 = \frac{4}{\kappa_0^2}C_t\,\mathrm{e}^{-u_{i0}/k_{\mathrm{B}}T}\,\mathrm{e}^{\Phi_0^{\mathrm{S}}}. \tag{53}$$

Substituting here the expression for the zeroth approximation of the surface potential Φ_0^{S}, Equation (37), one obtains extension of Davies isotherm (38), $\Gamma_{\mathrm{s}0} = K_0 C^{2/3}$, accounting for ion specific interactions:

$$\Gamma_{\mathrm{s}} = K_0\,\mathrm{e}^{-u_{i0}/2k_{\mathrm{B}}T}\,C^{2/3} \equiv KC^{2/3}. \tag{54}$$

Here C is the mean activity (32). Based on Equation (54) and the expression (39) for the non-specific adsorption constant K_0, one finds the expression for the *ion specific* adsorption constant K:

$$K = K_0\,\mathrm{e}^{-u_{i0}/2k_{\mathrm{B}}T} = \left(4K_{\mathrm{s}}/\kappa_0^2\right)^{1/3}\mathrm{e}^{-u_{i0}/2k_{\mathrm{B}}T}. \tag{55}$$

This procedure allows also the determination of the first iteration for the surface potential Φ^{S}. To do so, the equation of state (36) is used, with Γ_{s} given by Equation (54). After solving the result with respect to Φ^{S}, one obtains

$$\Phi^{\mathrm{S}} = \frac{1}{3}\ln\frac{\kappa_0^2 K_{\mathrm{s}}^2}{4} - \frac{1}{3}\ln\frac{C_{\mathrm{s}}^2}{C_{\mathrm{t}}} + \frac{u_{i0}}{2k_{\mathrm{B}}T}. \tag{56}$$

The comparison of Equations (54) and (56) with the respective zeroth (non-specific) approximations for the surface potential Φ_0^{S}, Equation (37), and the adsorption $\Gamma_{\mathrm{s}0}$, Equation (38), leads to

$$\Gamma_{\mathrm{s}} = \Gamma_{\mathrm{s}0}\exp(-u_{i0}/2k_{\mathrm{B}}T), \qquad \Phi^{\mathrm{S}} = \Phi_0^{\mathrm{S}} + u_{i0}/2k_{\mathrm{B}}T. \tag{57}$$

Note that the procedure is applied to the equation of state (36) of an "ideal" monolayer. For other systems in which the surfactant molecules interact directly with each other (e.g., with van der Waals or steric forces), it is possible that other system parameters are affected.

In Equation (52), it is assumed that the surface charge density is due to the surfactant ions only (i.e., it is $e_{\mathrm{s}}\Gamma_{\mathrm{s}}$). In reality, the counter-ions can penetrate also in the adsorbed layer, in the empty spaces between the surfactant heads, but, because of the relatively low values of the specific adsorption energies u_{i0} (cf. Table 2),

they do not remain firmly bound (unlike the surfactant ions) to the interface. Hence, most common ions must be treated as part of the diffuse layer. This was proven directly by Shimamoto and team [21], who studied experimentally by total-reflection X-ray absorption fine structure the ion distribution in the adsorbed and the diffuse layer.

2.3.2. Specific Interaction between an Ion and the Interface

The adsorption potential of the counter-ion u_{i0} is related to a number of parameters, among them: the molecular or ion static polarizabilities, $\alpha_{\mathrm{p,w}}$ and $\alpha_{\mathrm{p},i}$, and the ionization potentials I_{w} and I_i of the water molecule and the counter-ion, as well as the radii of the hydrated and bare ion (R_{h} and R_{b} respectively). These parameters are not always available and even when they are, they are not very reliable. As shown in Ref.[26], the adsorption energy u_{i0} depends strongly on the choice of the parameters and can vary by orders of magnitude. When several values of a given parameter were available in the literature, all were tested and the one giving best coincidence with the experimental data was retained.

In Ref.[26], the calculation of the energy u_{i0} was performed, using the London expression for the intermolecular potential u_{ij} between molecules of type i and j at a distance r_{ij} [42]:

$$u_{ij} = -L_{ij} / r_{ij}^6, \tag{58}$$

Where the London constant L_{ij} is related to the static polarizbilities $\alpha_{\mathrm{p},i}$ and $\alpha_{\mathrm{p},j}$ and the ionization potentials I_i and I_j of the interacting species:

$$L_{ij} = \frac{3\alpha_{\mathrm{p},i}\alpha_{\mathrm{p},j}}{2}\frac{I_i I_j}{I_i + I_j}. \tag{59}$$

Upon adsorption, the counter-ion displaces an ensemble of N_{w} water molecules (Figure 3). In the initial state (before adsorption), the ion is in the bulk and has energy u_i^{B} and the N_{w} water molecules are at the interface, with total energy $u_{\mathrm{w}}^{\mathrm{S}}$ (subscript indices "i" and "w" stand for "ion" and "water", superscript indices "S" and "B" stand for "surface" and "bulk", see Figure 3). In the final state (adsorbed ion), the ion and the water molecules have exchanged positions and their energies became u_i^{S} and $u_{\mathrm{w}}^{\mathrm{B}}$ respectively. Thus, the ion adsorption energy u_{i0}, which is equal to the change of energy upon adsorption, is:

$$u_{i0} = \left(u_i^{\mathrm{S}} - u_i^{\mathrm{B}}\right) - \left(u_{\mathrm{w}}^{\mathrm{S}} - u_{\mathrm{w}}^{\mathrm{B}}\right). \tag{60}$$

The hydration shell of the large ions is loose because they have lower hydration numbers n_{w} and larger area of the bare ion. That is why it is assumed that when they are adsorbed, the hydration shell is deformed by the interface as shown in Figure 3. Hence, they can approach the interface up to a distance equal to the radius R_{b} of the bare ion. We will refer to them as "type I ions". Smaller ions ("type II") have denser adsorption shell which cannot be rearranged upon adsorption, so that most probably they will remain immersed in water, along with their hydration layer. Therefore, they can approach the interface only to distances equal to R_{h}.

We will calculate first the energy u_i^{S} of the type I ions. Toward this aim, the London potential (58) is integrated over the volume of the water phase excluding the hydration shell, with r_{ij} being the distance between the volume element d$\boldsymbol{r}$ and the ion positioned at $r = 0$, $z = 0$ (that is, the integration is over $z > -R_{\mathrm{b}}$ and $r^2 + z^2 < R_{\mathrm{h}}^2$). The integration is performed in cylindrical coordinates:

$$u_i^{\mathrm{S}} = -\int_{-R_{\mathrm{b}}}^{R_{\mathrm{h}}} \int_{\sqrt{R_{\mathrm{h}}^2 - z^2}}^{\infty} \frac{L_{i\mathrm{w}} \rho_{\mathrm{w}} 2\pi r \mathrm{d}r \mathrm{d}z}{\left(r^2 + z^2\right)^3} - \int_{R_{\mathrm{h}}}^{\infty} \int_{0}^{\infty} \frac{L_{i\mathrm{w}} \rho_{\mathrm{w}} 2\pi r \mathrm{d}r \mathrm{d}z}{\left(r^2 + z^2\right)^3} = -\frac{2\pi}{3} \frac{L_{i\mathrm{w}} \rho_{\mathrm{w}}}{R_{\mathrm{h}}^3} \left(1 + \frac{3}{4} \frac{R_{\mathrm{b}}}{R_{\mathrm{h}}}\right); \tag{61}$$

here ρ_{w} is the particle density of water. Similarly, the bulk energy of the ion is (integration in spherical coordinates)

$$u_i^{\mathrm{B}} = -\int_{R_{\mathrm{h}}}^{\infty} \frac{L_{i\mathrm{w}}}{r_{i\mathrm{w}}^6} \rho_{\mathrm{w}} 4\pi r_{i\mathrm{w}}^2 \mathrm{d}r_{i\mathrm{w}} = -\frac{4\pi}{3} \frac{L_{i\mathrm{w}} \rho_{\mathrm{w}}}{R_{\mathrm{h}}^3}. \tag{62}$$

The respective energies of the ensemble of water molecules (assumed a sphere of radius R_{h}, or a part of it) are:

$$u_{\mathrm{w}}^{\mathrm{S}} = -\frac{2\pi}{3} \frac{L_{\mathrm{ww}} \rho_{\mathrm{w}}}{R_{\mathrm{h}}^3} \left(1 + \frac{3}{4} \frac{R_{\mathrm{b}}}{R_{\mathrm{h}}}\right); \qquad u_{\mathrm{w}}^{\mathrm{B}} = -\frac{4\pi}{3} \frac{L_{\mathrm{ww}} \rho_{\mathrm{w}}}{R_{\mathrm{h}}^3}. \tag{63}$$

Substituting Equations (61)-(63) into the expression (60) for u_{i0}, one obtains an explicit relation of the adsorption energy with the ionic properties of type I ions:

$$u_{i0} = \left(1 - \frac{3}{4} \frac{R_{\mathrm{b}}}{R_{\mathrm{h}}}\right) \frac{2\pi}{3} \frac{\rho_{\mathrm{w}}}{R_{\mathrm{h}}^3} \left(L_{i\mathrm{w}} - L_{\mathrm{ww}}\right). \tag{64}$$

To calculate u_{i0} for type II ions, one must set $R_{\mathrm{h}} = R_{\mathrm{b}}$ in Equation (64), which simplifies the expression to

$$u_{i0} = \frac{\pi}{6} \frac{\rho_{\mathrm{w}}}{R_{\mathrm{h}}^3} \left(L_{i\mathrm{w}} - L_{\mathrm{ww}}\right). \tag{65}$$

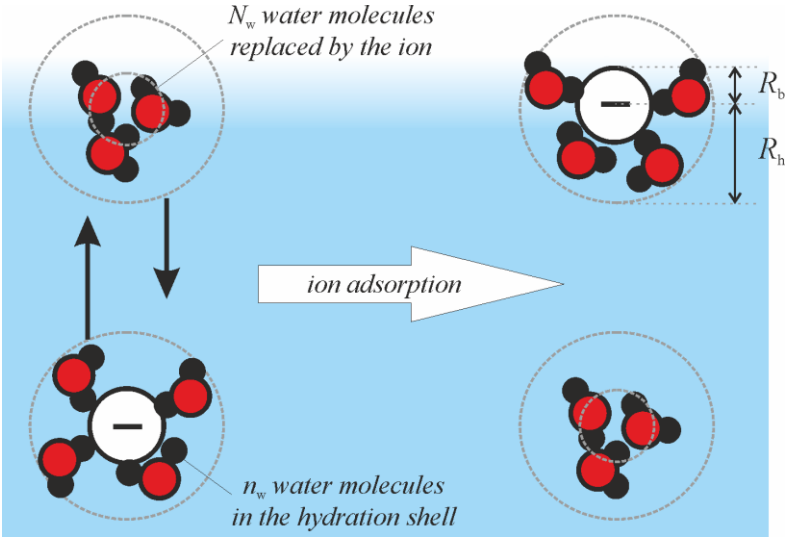

Figure 3. Scheme of the process of adsorption of a type I ion. *Left*: ion in the bulk. *Right*: ion at the surface. The n_{w} hydrating water molecules might be pushed away by the interface, so that the shortest distance of

approach of the ion to the interface is the bare ion radius R_b. Upon adsorption, the ion replaces an ensemble of N_w water molecules. For type II ions, the shortest distance of approach of the ion to the interface is the hydrated ion radius R_h.

The values of the hydration number n_w and the radius R_h of the hydrated ion depend strongly on the method used for their determination and can vary widely [43]. It seems that more reasonable results can be obtained by model calculations, rather than experimentally. For monovalent ions, Marcus [44] found that the hydration number n_w can be represented by the empirical relation

$$n_w = A_v/R_i, \tag{66}$$

where $A_v = 3.6$ Å for all ions. He further assumed that the hydrating n_w water molecules, considered as spheres with radius $R_w = 1.38$ Å and volume $v_w = 11$ Å^3, are squeezed around the ion, forming a layer of thickness $R_h - R_b$ and volume:

$$n_w v_w = \frac{4\pi}{3}\left(R_h^3 - R_b^3\right). \tag{67}$$

The last relation is used to calculate R_h. The values of n_w and R_h calculated in this way [26, 44, 45] are shown in Table 2. Robinson and Stokes (Equation (9.27) in Ref. [33] used similar approach, but with water molecular volume $v_w = 30$ Å^3, which follows from the density of water. They also used different values of the hydration number n_w, which were calculated from the ion diffusivity (see Table 11.10 in Ref. [33]. Ivanov and team [26] calculated the radius R_h using both sets of parameters; for the ions of interest the results for R_h did not differ much from each other. Both sets of R_h, those calculated by the method of Marcus and by the method of Robinson and Stokes, differ however much from the often quoted values (e.g. [42]) $R_h = 3.8, 3.6, 3.3$ Å for Li^+, Na^+ and K^+, and 3.5, 3.3 and 3.3 Å for F^-, Cl^- and Br^- respectively.

The London constants L_{iw} for the interaction ion-water molecule, and L_{ww} for the interaction of N_w water molecules with a single water molecule are calculated directly from Equation (59):

$$L_{iw} = \frac{3\alpha_{p,i}\alpha_{p,w}}{2}\frac{I_i I_w}{I_i + I_w}, \qquad L_{ww} = \frac{3}{4}N_w\alpha_{p,w}^2 I_w. \tag{68}$$

For the calculation of L_{ww}, the ensemble of N_w water molecules is regarded as a sphere with polarizability $N_w\alpha_{p,w}$ [26]. The number N_w was assumed equal to the ratio between the volume of the bare ion and the volume of one water molecule [46]:

$$N_w = R_b^3 / R_w^3, \tag{69}$$

Where, R_w is the radius of the water molecule. For the value of R_w, two possibilities were tested in Ref.[26]: (**i**) the average volume per molecule (30 Å^3), based on the water density, yields $R_w = 1.93$ Å; and (**ii**) the proper volume of a water molecule, 11 Å^3, corresponds to $R_w = 1.38$ Å. Better agreement with the experimental data was obtained with the second option, $R_w = 1.38$ Å. The used value of the static polarizability of water was $\alpha_{p,w} = 1.48$ Å^3 and of the ionization potential was $I_w = 2.02\times10^{-18}$ J [47].

The values of the ionization potentials of the ions I_i are also questionable. In Ref.[26], the ionization potential in vacuum was used for halogen ions. For the alkaline ions, it was corrected for the hydration effect, although the correction was small. Later we found some new data about the system parameters which showed that the hydration correction is even smaller and hereafter it was disregarded. For the cations, we used the second ionization potential, since the first one corresponds to ionization of the respective atom, not ion. Since the anions have already accepted one extra electron, their ionization potential must be equal to the negative value of the electron affinity.

Table 2. Specific adsorption energies of the considered ions ($T = 25°C$). R_b – bare ion radius; n_w – hydration number, Equation (66); R_h – hydrated ion radius, Equation (67); N_w – number of water molecules in the ensemble, replaced by the ion upon adsorption, Equation (69); L_{ww} – London constant of this ensemble, Equation (68); $\alpha_{p,i}$ – polarizability of the ion; I_i – second ionization potential of the cations and negative electron affinity of the anions; u_{i0} – ion specific adsorption energy, Equation (65) for type I ions (no deformation of the hydration shell) and Equation (64) for type II ions (with deformation of the hydration shell). The ions in the Table are ordered by increasing absolute values of u_{i0}. The sequence of both cations and anions is the same as in Hofmeister series, but for the cations this order corresponds to increasing efficiency as opposite to the series. Source data: Marcus [44]; Nikolskij [47]; Tavares [16]; Dietrich [48]; Lide [49].

Cation	R_b [Å]	n_w Eq (66)	R_h [Å] Eq (67)	N_w Eq (69)	L_{ww} Eq (68) [m^{6}J] ×10^{80}	$\alpha_{p,i}$ [Å^3]	I_i [J] ×10^{18}	L_{wi} Eq (68) [m^{6}J] ×10^{80}	u_{i0}/k_BT type I Eq (64)	u_{i0}/k_BT type II Eq (65)
Li^+	0.69[1]	5.22	2.41	0.13	41.5	0.03[1]	12.1[2]	11.5		–0.09
Na^+	1.02[1]	3.53	2.18	0.40	134	0.15[3]	7.58[2]	53.1		–0.33
NH_4^+	1.53[4]	2.35	2.14	1.36	453	1.64[1]	2.13[2]	378	–0.61	
K^+	1.41[1]	2.55	2.12	1.07	354	0.79[3]	5.07[2]	253	–0.90	
Rb^+	1.65[5]	2.18	2.17	1.71	568	1.4[1]	4.41[2]	431	–0.98	
NMe_4^+	2.80[1]	1.29	2.94	8.36	2770	9.08[1]	2.43[2]	2220	–1.05	
Anion	**R_b [Å]**	**n_w**	**R_h [Å]**	**N_w**	**L_{ww} [m^{6}J] ×10^{80}**	**$\alpha_{p,i}$ [Å^3]**	**I_i [J] ×10^{18}**	**L_{wi} Eq (68) [m^{6}J] ×10^{80}**	**u_{i0}/k_BT type I**	**u_{i0}/k_BT type II**
Ac^-	1.65[1]	2.18	2.17	1.71	568	5.50[1]	0.544[1]	545		–0.185
OH^-	1.33[1]	2.71	2.11	0.90	297	2.04[1]	0.345[1]	134		–0.736
F^-	1.33[1]	2.71	2.11	0.90	297	1.04[2]	0.545[1]	99.1		–0.891
Cl^-	1.64[1]	2.20	2.17	1.68	557	3.59[2]	0.580[1]	359	–1.43	
Br^-	1.95[1]	1.85	2.31	2.82	937	5.07[2]	0.540[1]	480	–2.32	
NO_3^-	2.00[1]	1.80	2.33	3.05	1010	3.93[1]	0.631[1]	420	–2.83	
N_3^-	1.95[1]	1.85	2.31	2.82	937	4.45[1]	0.444[1]	360	–2.93	
ClO_4^-	2.40[1]	1.50	2.61	5.26	1750	5.25[2]	0.758[1]	642	–3.28	
BF_4^-	2.30[1]	1.57	2.53	4.63	1540	2.80[1]	0.902[1]	388	–3.84	

Eq-Equation

2.4. Comparison with Experiment

2.4.1. Experimental Verification of the Theory of K

Our expression (12) for the adsorption energy E_a differs from Equation (4.3) of Davies and Rideal [24] by the presence of the new term $\sigma_0\alpha_\perp$.

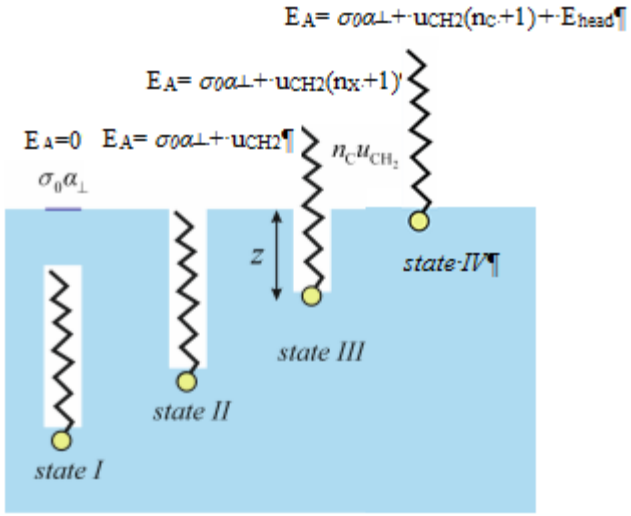

Figure 1. Four different stages from the adsorption of the surfactant molecule on gas|water interface: Stage I - Prior the very adsorption; Stage II - The cap of the hydrocarbon tail touches the gas|water interface; Stage III - Part of the hydrocarbon tail with n_x carbon atoms penetrated into the air's phase; Stage IV - The whole hydrocarbon tail with n_c carbon atoms penetrated into the air's phase.

This term stems from the disappearance of area $\alpha_\perp$ of interfacial tension σ_0 when the surfactant molecule is adsorbed at the interface. To demonstrate the significance of this energy, we will analyze the data by Rehfeld [39] and Gillap team [50] for the adsorption of $C_{12}H_{25}SO_4Na$ at various oil|water interfaces, where the oil phase is varied – this is the only simple way to change the interfacial tension σ_0 of the clean surface without affecting too much the other parameters of Equation (12), and allows direct observation of the expected effect of σ_0 on K.

Substituting the expression (6) for K_s into the definition (55) of K, and using the result (12) for the adsorption energy E_a, one obtains

$$\ln K + \frac{u_{i0}}{2k_BT} \equiv \ln K_0 = const + \frac{u_{CH_2}}{3k_BT} n_C + \frac{\alpha_\perp}{3k_BT}\sigma_0, \tag{70}$$

Where,

$$const = \frac{E_{head}}{3k_BT} + \frac{\alpha_\perp u_{CH_2}}{3a_pk_BT} + \frac{1}{3}\ln\frac{4\delta_a}{\kappa_0^2}. \tag{71}$$

In Equation (70), we preferred to correct the experimental adsorption constant K with the term $u_{i0}/2k_BT$ standing for the ion specific adsorption energy of Na^+ ion ($u_{i0} = -0.34\times k_BT$, cf. Table 2), in order to obtain the counterion-independent constant K_0, Equation (39).

The effect of the nature of the hydrophobic phase is twofold. First (and more important), the change of the oil will affect σ_0 in the last term in Equation (70). The interfacial tension σ_0 of the pure oil|water interfaces in Rehfeld's experiments ranges from 31.3 mN/m for 1-hexene|water to 53.2 mN/m for water|heptadecane. According to Equation (70), this corresponds to a difference of about 0.4 in the value of $\ln K_0$. The second effect of the hydrophobic phase is on the transfer energy u_{CH_2}, which also depends to a certain extent on the nature of the oil. According to Tanford [30], for transfer of a $-CH_2-$ group from water to hydrocarbons, u_{CH_2} does not differ significantly for alkanes and alkenes. Aveyard and Briscoe [51] found only a weak dependence of u_{CH_2} on the length of the alkanes. We could not find data for the aromatic and cyclic compounds used by Rehfeld, but the relatively good coincidence between theoretical dependence and experimental values depicted in Figure 5 suggests that this second effect is smaller. Therefore, for all considered systems, only the term $\sigma_0\alpha_\perp$ in Equation (70) will vary significantly with the nature of the oil.

Three typical surface pressure isotherms $\pi^S(C^{2/3})$ for oils of different interfacial tensions σ_0, based on the data of Rehfeld [39], are shown in Figure 4. From these data, the values of K were determined according to Equation (46) and corrected with $u_{i0}/2k_BT$ according to Equation (70) to obtain the counterion-independent quantity $\ln K_0$. The obtained $\ln K_0$ values for several different oils with the same surfactant $C_{12}H_{25}SO_4Na$ are plotted in Figure 5 in coordinates $\ln K_0$ vs. σ_0. The line is plotted according to Equation (70) with the theoretical slope $\alpha_\perp / 3k_BT$ = 0.0172 m/mN, corresponding to the value $\alpha_\perp$ = 21.2 Å^2 given by Tanford [30] for the hydrocarbon chain cross-sectional area. The theoretical intercept, determined from Equations (70) and (71) is 4.8. Its experimental value, from Figure 5, is 4.16±0.08, which is reasonably close to the theoretically predicted. These data confirm our theory of the adsorption energy and thickness, Equations (12) and (15).

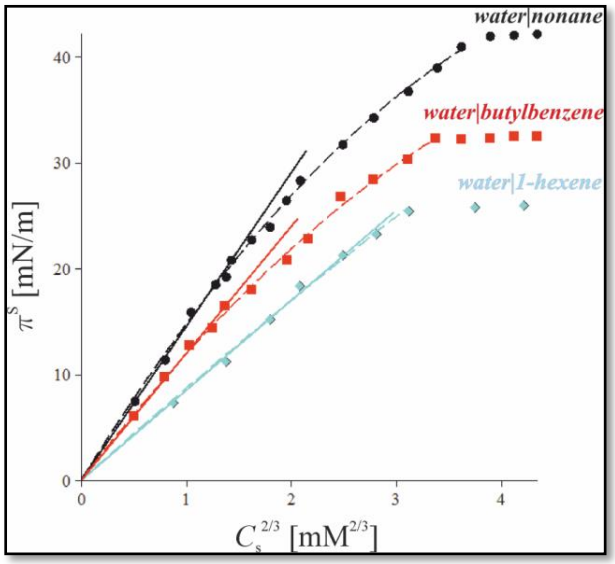

Figure 4. Surface pressure π^S vs. 2/3-power of surfactant concentration $C_s^{2/3}$ for adsorption of $C_{12}H_{25}SO_4Na$ at oil|water for three typical oils with different interfacial tensions (σ_0 = 50.9, 40.1 and 31.3 mN/m for nonane|watere, butylbenzene|water and 1-hexene|water respectively). Experimental data by Rehfeld [39], T = 25°C. Solid line: the linear dependence (38); dashed line: fit with quadratic polynomial, Equation (46), up to CMC. From the polynomial dependences, the adsorption constants K, used in Figure 5, are determined.

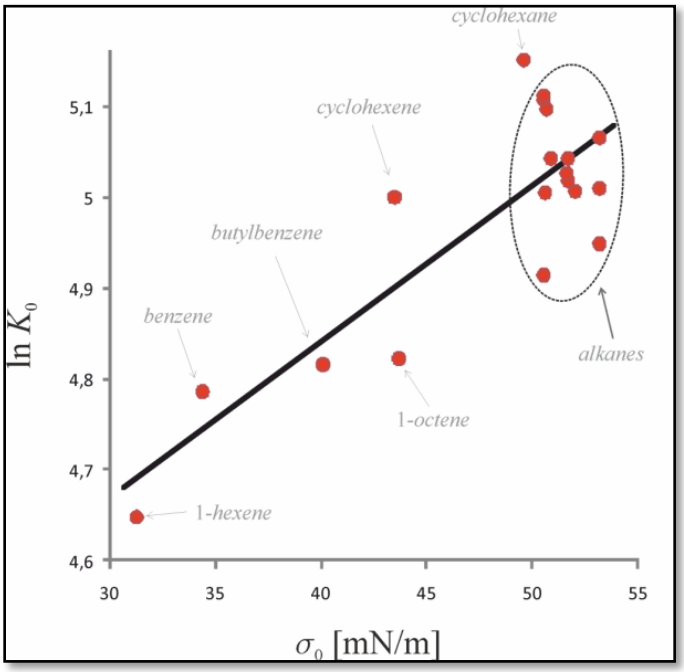

Figure 5. Dependence of $\ln K_0$ of $C_{12}H_{25}SO_4Na$ on the interfacial tensions σ_0 of the pure oil|water interfaces. All points are determined from plots similar to those in Figure 4. The values of K were calculated from quadratic fit of π^S vs. $C_s^{2/3}$, Equation (46), and were corrected for the counter-ion effect according to Equation (70) to yield K_0. Solid line: theoretical dependence (70), with the theoretical slope $\alpha_\perp / 3k_BT$ = 0.0172 m/mN (cf. Equation (70)), corresponding to $\alpha_\perp$ = 21.2 Å^2 [30]. The intercept is 4.16±0.08.

We now turn to the dependence of the adsorption constant K on the number of carbon atoms n_C in the hydrophobic tail of homologous surfactants. As it is obvious from Figure 6, the addition of –CH_2– groups leads to a strong increase of the surface pressure π^S, which is related, according to Equation (70), to the energy u_{CH_2} of transfer of a –CH_2– group from water to the hydrophobic phase. Both Tanford [30] and Davies and Rideal (Table 4-I in Ref.[24]) cite different values of u_{CH_2} for oil|water and air|water. For water|alkane interface, Tanford gives $u_{CH_2}^{WO} = 5.75 \times 10^{-21}$ J vs. $u_{CH_2}^{WO} = 5.98 \times 10^{-21}$ J by Davies and Rideal. For W|G, Tanford gives $u_{CH_2}^{WG} = 4.35 \times 10^{-21}$ J. Davies and Rideal found that $u_{CH_2}^{WG}$ depends on the coverage: for dilute monolayers, $u_{CH_2}^{WG} = 4.17 \times 10^{-21}$ J, while for denser monolayers (90Å^2 per molecule) $u_{CH_2}^{WG} = 4.85 \times 10^{-21}$ J.

We will compare the value of K_0 of homologous series of surfactants at different oil|water interfaces – different oil phases and different σ_0. To analyze the effect from the chain length n_C, we reduced all K values to standard clean interfacial tension $\sigma_0^{\text{alkane}} \equiv 52$ mN/m; the standardized value K_0^{alkane} is easily recalculated by using Equation (70),

$$\ln K_0^{\text{alkane}} - \ln K_0 = \frac{\alpha_\perp}{3k_B T}\left(\sigma_0^{\text{alkane}} - \sigma_0\right). \qquad (72)$$

K_0^{alkane} is the expected adsorption constant of the surfactant at the water|alkane interface, provided that $u_{CH_2}^{WO}$ of the investigated oil is the same as for alkanes (cf. the discussion below Equation (71)). The data for adsorption of sodium alkylsulfates and alkyltrimethylammonium bromides at the oil|water, plotted in our Figure 7, are consistent with Equation (70). The value $u_{CH_2}^{WO} = 5.75 \times 10^{-21}$ J, quoted by Tanford, agree very well with the observed slope $\mathrm{d}K_0^{\text{alkane}} / \mathrm{d}n_C$ (which is equal to $u_{CH_2} / 3k_B T$, Equation (70)).

The adsorption of homologous series at the W|G in the LE region can be similarly analyzed (Figure 6b). We determined the adsorption constant *K* for each particular system by fitting the experimental data $\pi^S(C^{2/3})$ with Equation (46), $\pi^S = \pi_0 + 3k_B TKC^{2/3} + bC^{4/3}$. We considered only the parts of the surface tension isotherms corresponding to LE state of the adsorption layers. The dependence of $\ln K_0$ on n_C for the LE monolayers at the air|water interface is once again linear, as shown in Figure 7, so Equation (70) is valid. Surprisingly, within the experimental error, the slope is the same as for oil|water. According to Langmuir hypothesis, this is certainly due to the fact that the transfer of a –CH_2– group is a transfer from water to liquid expanded adsorption layer (and not to a gas!), which is nearly equivalent to transfer from water to oil. We found it hard to estimate the corresponding energy of transfer from water to gaseous monolayers, due to the insufficient and contradictory data for the adsorption in this region. One can expect, however, that $u_{CH_2}^{WG}$ will have lower value (about 4.17 to 4.35 $\times$ 10^{-21}.

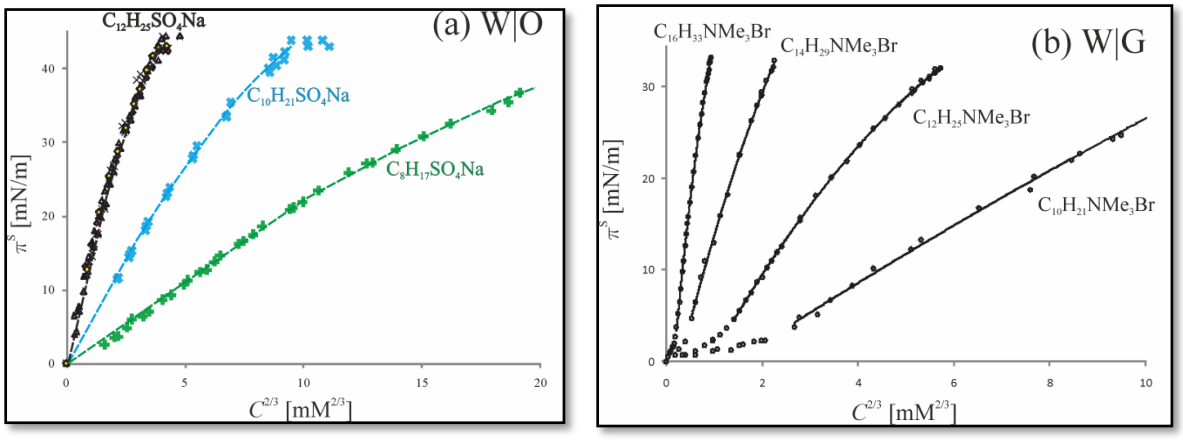

Figure 6. Dependence of the surface pressure π^S vs. 2/3-power of the mean activity, $C^{2/3}$. **(a)** Alkylsulfates of different chain length at the oil|water, with or without added NaCl. The data for $C_{12}H_{25}SO_4Na$, with various

amounts of NaCl, are the same as in Figure 1; the data for $C_8H_{17}SO_4Na$ and $C_{10}H_{21}SO_4Na$ at the decane|water interface are with added 50÷500 mM NaCl [52]. The data were processed as in Figure 4: dashed lines are quadratic fits with Equation (46). **(b)** Alkyltrimethylammonium bromides of different chain length at the air|water. The data for $C_{10}H_{21}NMe_3Br$ are with 0÷10 mM NaBr [18]; data for $C_{12}H_{25}NMe_3Br$, $C_{14}H_{29}NMe_3Br$ and $C_{16}H_{33}NMe_3Br$ are by Aratono. Solid lines correspond to quadratic fits, Equation (46). From the fits, the values of the adsorption constants K were obtained; the final result is the experimental dependence of K on the number of carbon atoms n_C in the hydrophobic tail, plotted in Figure 7.

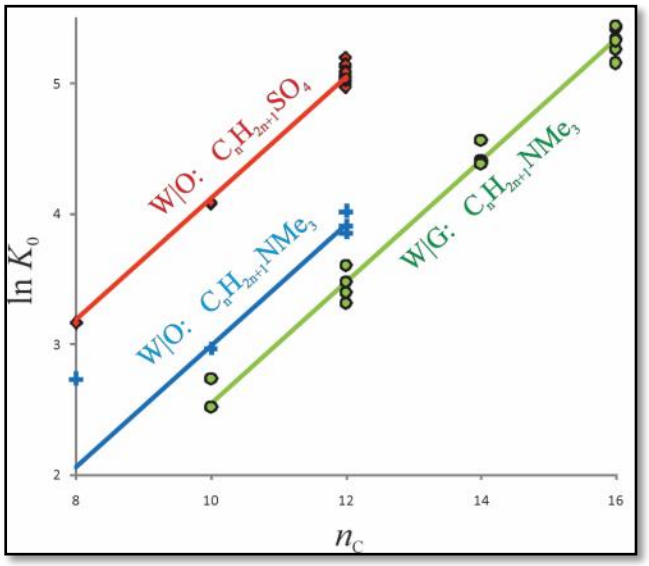

Figure 7. Dependence of the logarithm of the adsorption constant $\ln K_0$ on the number of carbon atoms n_C in the hydrocarbon chain. Circles: data for alkylsulfates at the W|O; the values of K_0 were calculated from $\pi^S(C_s^{2/3})$ dependences similar to those shown in Figure 6. The data for $C_{12}H_{25}SO_4Na$ are from the same sources as in Figure 5; data for $C_8H_{17}SO_4Na$ and $C_{10}H_{21}SO_4Na$ are with 0÷500 mM NaCl, and the oil is either decane [52] or other alkanes [50]. Correction for σ_0 was made, and all data were reduced to σ_0 = 52 mN/m according to Equation (72). Crosses: adsorption of alkyltrimethylammonium salts at W|O. Data for $C_8H_{17}NMe_3$ and $C_{10}H_{21}NMe_3$ are with decane in the presence of 0÷500 mM NaCl [52]; data for $C_{12}H_{25}NMe_3Br$ and Cl is with hexane, hexadecane and petroleum ether and 0÷500 mM NaCl [52]. Diamonds: data for the adsorption of alkyltrimethylammonium bromides and chlorides at the W|G, with various amounts of salt [18], [53]. Lines – the theoretical dependence (70) with $u_{CH_2} = 5.75 \times 10^{-21}$ J as given by Tanford [30]. The intercepts were determined as fitting parameters: –0.55 for alkylsulfates at W|O, for alkyltrimethylammonium salts at W|O: –1.63, and at W|G: –2.12.

On Figure 8, the surface pressure isotherm of four $C_{12}H_{25}NMe_3^+$ salts at W|G is shown. Obviously, the counter-ion can drastically increase the surface activity of the surfactant ion, and the effect of the counter-ion follows Hofmeister series. Similar curves were obtained for the other surfactants, considered below. Our aim now is to demonstrate how the results in Figure 8 can be explained quantitatively with the model developed in Section 0.

Equation (55) can be presented in logarithmic form:

$$\ln K = \ln K_0 - \frac{1}{2}\frac{u_{i0}}{k_B T}. \qquad (73)$$

We already discussed the first term in the right hand side of this equation: it can be estimated with Equations (70) and (71). In comparison with these equations, Equation (73) accounts additionally for the effect of the counterion specific adsorption energy u_{i0}.

To validate Equation (73) experimentally, several cases with data for surface tension of the same ionic surfactant with different counteri-ons (with or without added salt) were analyzed. We found only scarce experimental data for such systems for the same surfactant ion. In order to supplement these data with variety of counter-ions, we used the established relation (70) between K_0 and the number of carbon atoms n_C: using it, we were able to reduce *K* of any surfactant from a homologous series to a standard constant K_{12} for surfactant with $n_C = 12$:

$$\ln K_{12} = \ln K - \frac{u_{CH_2}}{3k_B T}(n_C - 12), \qquad (74)$$

where $u_{CH_2} / k_B T$ has a value between 0.96 and 1.26 depending on the surfactant's hydrophilic head [31]. For homologous series of surfactants with the same ionic head at the same interface and temperature, this standard constant K_{12} should depend on u_{i0} only, cf. Equations (70) and (71).

The specific adsorption energies u_{i0} of the ions were taken from Table 2. The values of K were found by curve-fitting with the quadratic dependence Equation (46). The so-found values of K were used to calculate the non-specific adsorption constant K_0 for each of the surfactant ions through Equation (73). In agreement with the theory, the obtained values of ln K_0 are the same for a given surfactant ion with any respective counter-ion.

The dependence of the adsorption constant on the adsorption energy u_{i0} of the counter-ion is illustrated in Figure 9, where $\ln K_{12}$ vs. $-u_{i0}/k_B T$ is plotted for three different surfactant ions. The lines are drawn according to Equation (73) by using the theoretical slope ½ and the average values of $\ln K_0$ for each surfactant ion: 4.80±0.13 for $C_{12}H_{25}SO_4^-$, 3.74±0.02 for $C_{12}H_{25}PyrNMe_2^+$, and $\ln K_0 = 3.28 \pm 0.10$ for $C_{12}H_{25}NMe_3^+$. The theory describes the data adequately. Note that the values of the adsorption energy u_{i0} listed in Table 2 were obtained without using any free adjustable parameter. The average values of $\ln K_0$ can be compared to the theoretical value $\ln K_0 = 5.8$, calculated by Equations (70) and (71) with neglected E_{head}. The difference between surfactants with the same tail but with different head-groups is clearly due to the head adsorption energy in Equation (12) [31]. From the experimental values of K_0, it can be calculated that E_{head} is of the order of -2.79, and $-5.85 \times k_B T$ for $-SO_4^-$ and $-NMe_3^+$ correspondingly [31].

We ordered below the counter-ions according to the experimental values of the adsorption constants K_{12} for a given surfactant ion in Figure 9:

$$Ac^- < F^- < Cl^- < Br^- \hat{} \ NO_3^- < BF_4^- \qquad \text{for cationic surfactants} \qquad (75)$$

$$Li^+ < Na^+ < NH_4^+ < Rb^+ \hat{} \ K^+ < NMe_4^+ \quad \text{for anionic surfactants} \tag{76}$$

.

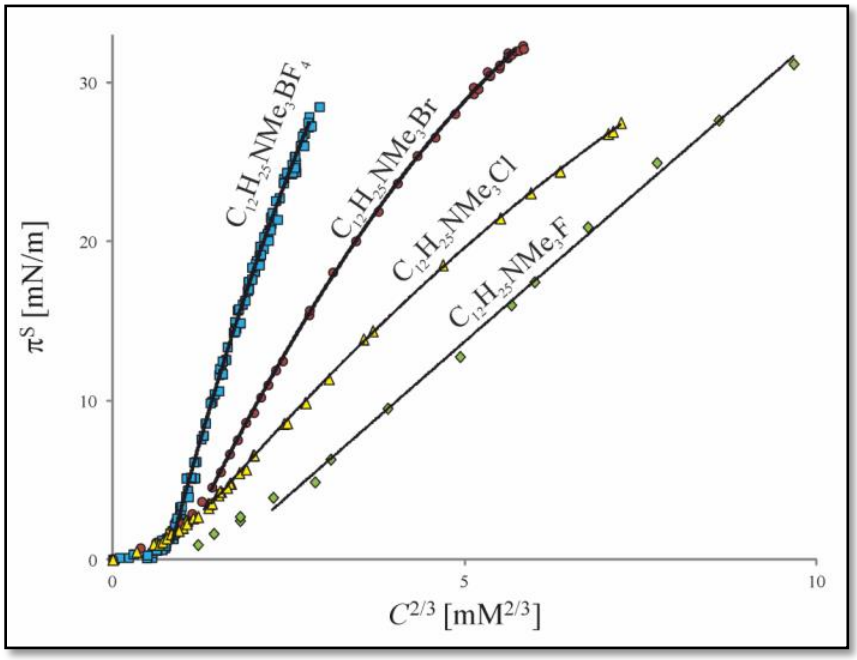

Figure 8. Surface pressure π^S vs. $C^{2/3}$(2/3-power of the mean activity) for $C_{12}H_{25}NMe_3$ salts. The surface pressure at a given concentration of these increases in accordance with Hofmeister series (BF_4^- > Br^- > Cl^- > F^-). The data for $C_{12}H_{25}NMe_3BF_4$ are with added 0÷15mM $NaBF_4$ [20]; $C_{12}H_{25}NMe_3Br^-$ and Cl^- are without additives [20, 29]; the data for $C_{12}H_{25}NMe_3F$ are obtained by 100 mM NaF added to 0÷15mM $C_{12}H_{25}NMe_3Br$ solutions [29]. $T = 23 \div 25^{\circ}C$. The lines are quadratic fits. The results were used for calculation of the respective adsorption constants K, used in Figure 9.

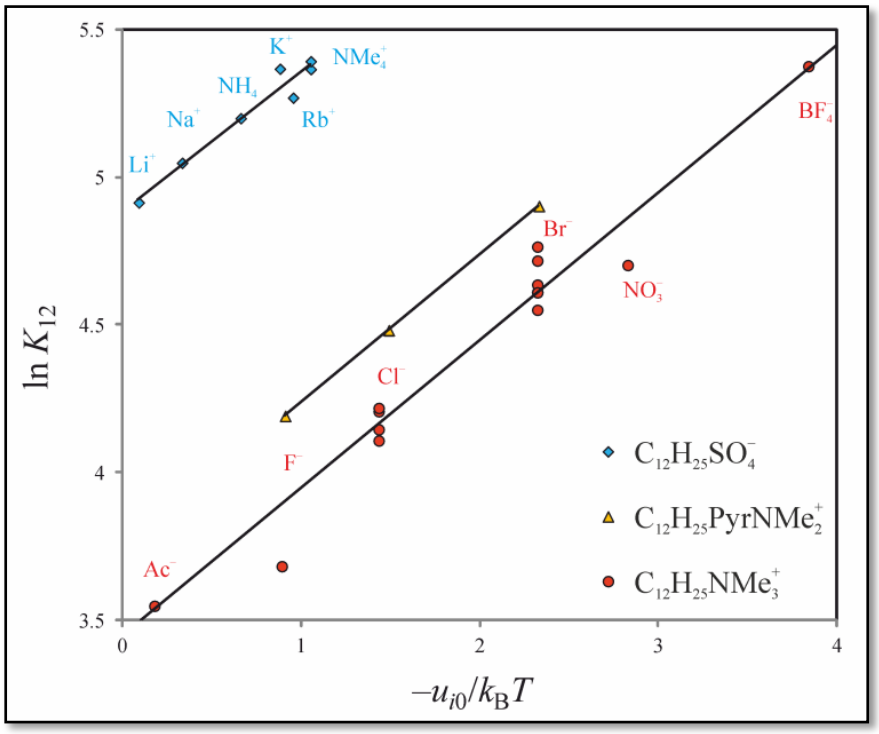

Figure 9. Dependence of the adsorption constant K_{12} on the ion adsorption energy $-u_{i0}/k_BT$ of surfactants with 3 different head groups at W|G. The values of K_{12} were determined from $\pi^S(C^{2/3})$ data as those in Figure 8. For this plot, we used the calculated values of u_{i0} from Table 2. Lines: comparison with the theoretical dependence with fixed slope ½, Equation (73). Sources: $C_{12}H_{25}SO_4^-$ with Li^+ alone [54, 55] and Li^+ with added 1 mM NH_4^+ [54]; for Na^+, cf. Figure 1; NH_4^+ and NMe_4^+ stand for 5÷10 mM NH_4^+ or NMe_4^+ with 1÷3 mM Li^+ [54]; K^+ and Rb^+ are without added salt [55]; $T = 23\div33^\circ C$. *K*-values for 1-dodecyl-4-dimethylaminopyridinium ($C_{12}H_{25}PyrNMe_2^+$) halogenides are calculated from Koelsch's data [56] (no added salt or 100mM NaF/NaCl/NaBr added to $C_{12}H_{25}PyrNMe_2Br$ at room temperature). $C_{12}H_{25}NMe_3^+$ is by Aratono (BF_4^- with added 0÷10 mM $NaBF_4$, NaCl, NaBr [20, 37] and Bergeron [53]. Data for $C_{10}H_{21}NMe_3^+$ (Br^- with 0÷10 mM NaCl [18, 53]), $C_{14}H_{29}NMe_3^+$ (Cl^- and Br^- [53]) and $C_{16}H_{33}NMe_3^+$ (Cl^- and Br^- in presence of 0÷100 mM salt [18, 53]; 10÷100 mM Ac^-, NO_3^- or F^- in the presence of 0÷0.5 mM Br^- [18]) is also used in this Figure – the corresponding adsorption constants K of these surfactants were reduced to the standard constant K_{12} of $C_{12}H_{25}NMe_3^+$ through Equation (74). All measurements with $C_nH_{2n+1}NMe_3^+$ were performed at $T = 20\div25^\circ C$.

The Hofmeister effect influences also the other parameters in the surface pressure isotherm (46). We found strong correlation between the spreading pressure π_0 of the surfactant and its counter-ion. In Figure 10, the spreading pressure of $C_nH_{2n+1}NMe_3^+$ salts is plotted against u_{i0}. The dependence is close to linear; the spreading pressure increases in absolute value with $-u_{i0}$.

The good coincidence between the theoretical dependence Equation (73) and experiment, demonstrated above, suggests that the effect of the type of counter-ions on the adsorption constant K is due not only to steric reasons, related to ion size, as it is sometimes assumed [57-59], but is also due to van der Waals interactions.

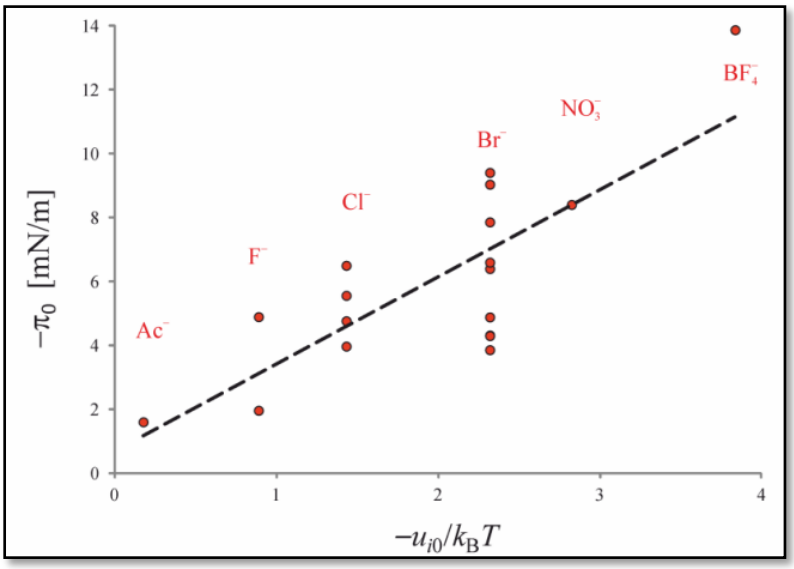

Figure 10. Hofmeister effect on Langmuir's spreading pressure π_0 of $C_nH_{2n+1}NMe_3^+$ salts at W|G: dependence of $-\pi_0$ on $-u_{i0}/k_BT$. The spreading pressure equals the intercept of quadratic fits of $\pi^S(C^{2/3})$ (cf. Figure 8). π_0 shows strong correlation to the ion adsorption energies u_{i0}. Data sources as in Figure 10.

3. Ion-Specific Effects on the Stability of Dispersed Systems and Relation to State of the Adsoprtion Layer

3.1. Surface Force Analysis

The ion-specific effects on the state of the adsorbed surfactant layer influence the stability of foams and emulsions. This section is devoted to the investigation of the type of the surfactants counter-ion on the stability of the dispersed systems. It presents the experimental data of Ref. [27] and such one conducted in the present work.

Ref. [27] presents experimental data on the disjoining pressure of water films in air (foam films) stabilized by 1 mM solutions of hexadecyltrimethylammonium bromide ($C_{16}H_{33}NMe_3Br$) and 9 mM added salt (NaF, NaCl, NaBr). The disjoining pressure, stabilizing the films, was measured in a thin film pressure balance by using the Mysels-Jones porous plate technique (Figure 12).

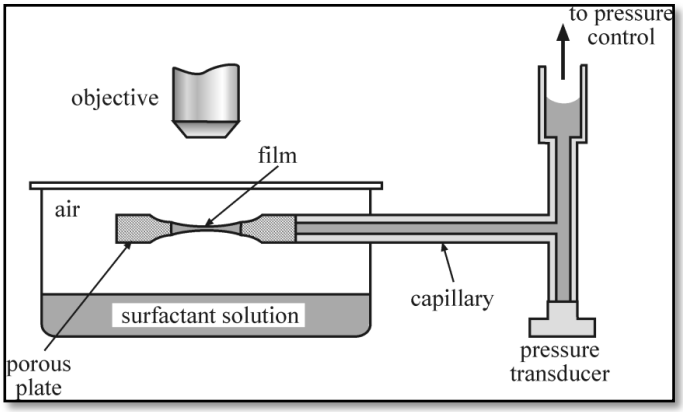

Figure 12. Schematic presentation of the porous plate cell.

The main question, which we raise is how the type of the counter-ions affect the stability of foams and emulsions. We know from the previous sections that the counter-ions with a higher absolute value of the specific adsorption on air|water or oil|water interfaces are integrated onto the surfactant adsorption layer in larger degree and vice versa. Hence, at a higher level of counter-ion adsorption the surface potential should be decreased more and vice versa. The theory of the electrostatic disjoining pressure has been developed by many authors, above all by Derjaguin and associates. Their results are summarized in the excellent book of Churaev [60]. According to their theory (neglecting the ion specific effects) the electrostatic disjoining pressure, Π_{el}, in a planar film of low surface potential or large thickness is given by the following expression:

$$\Pi_{el} = 64 k_B T C_t \tanh^2\left(\Phi_0^S / 4\right)\exp\left(-\kappa h\right) = \Pi_0 \exp\left(-\kappa h\right) \tag{77}$$

where C_t is total ion concentration. Since during the derivation of Equation (77) in Ref. [60] no other assumptions about the surface potential were done, we decided that in order to account for the specific effects it should be sufficient merely to replace Φ_0^S with Φ^S by means of the following equation:

$$\Phi^S = \Phi_0^S + u_0 / 2k_B T \tag{78}$$

Equation (77) suggests that the dependence of the experimental disjoining pressure Π on the thickness h should be close to linear in coordinates $\ln \Pi$ vs. h. Figure 13 shows that indeed this is the case. Since the films are rather thick, one can disregard the contribution of the van der Waals disjoining pressure (direct numerical calculations confirmed this). This permits identifying Π with Π_{el} and using Equation (77) for the calculation of Π, but with Φ^S replacing Φ_0^S. The lines in Figure 13 are almost parallel and obey the equation

$$\ln \Pi_{el} = \ln \Pi_0 - \kappa h \tag{79}$$

The obtained intercepts $\ln\Pi_0$ and slopes κ are shown in Table 2.

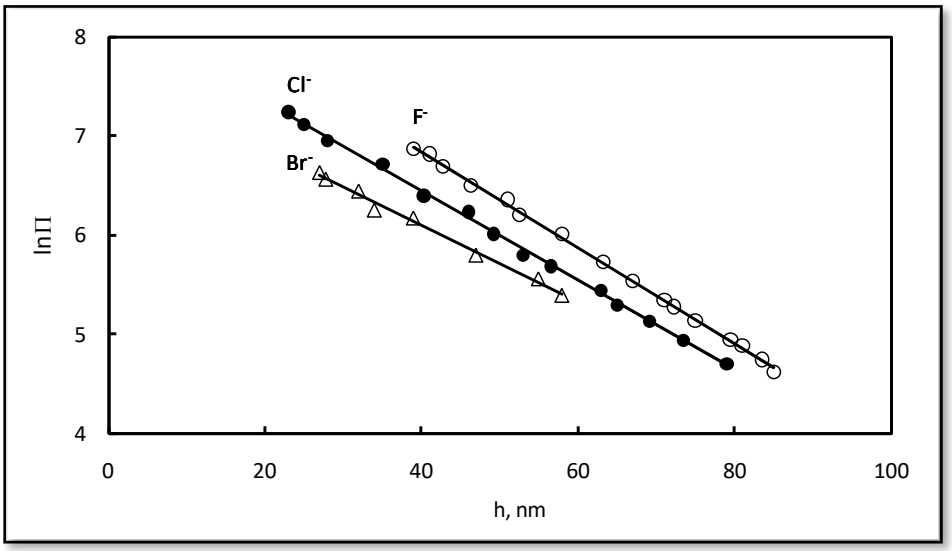

Figure 13. Plot of $\ln\Pi$ vs. h for foam films stabilized with $C_{16}H_{33}NMe_3Br$ and NaX (X = F^-, Cl^-, Br^-).

Table 3. Intercepts, $\ln \Pi_0$, and slopes, κ, of the lines in Figure 11.

Ion	F^-	Cl^-	Br^-
$\ln \Pi_0$ [Pa]	8.79	8.25	7.65
κ [nm^{-1}]	0.0485	0.0451	0.0386

The almost parallel, but shifted, lines suggest that the specific ion interactions (if any) are affecting mostly the surface potential Φ^S. By means of Equation (77) we calculated the experimental values of Φ^S from the obtained data for Π_0 (see Table 3) and plotted in Figure 14 the results as Φ^S vs. $-u_0/k_BT$. The relatively good linearity and close value of the experimental slope, 0.4, to the theoretical one, 1/2, (cf. Equation (78)) seem to confirm the role of the ion specific effect.

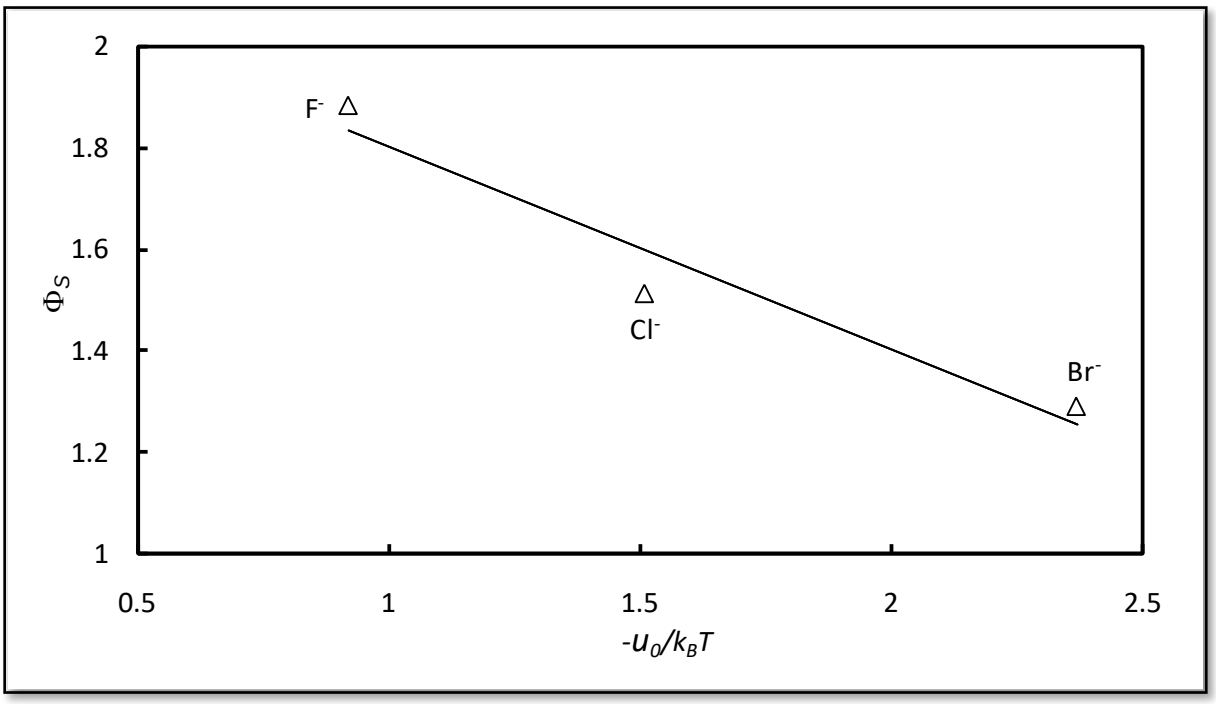

Figure 14. Combined surface potential Φ^S vs. $-u_0/k_BT$ for foam films stabilized with $C_{16}H_{33}NMe_3Br$ + NaX (X = F^-, Cl^-, Br^-). The slope is –0.4.

The Hofmeister effect on the surface potential and the disjoining pressure, Π, is by no means negligible. To setimate it for films closer to reality, in Figure 15 we present the results (obtained in Ref. [26]) for the total disjoining pressure Π_{total} (including also the van der Waals contribution with Hamaker constant $A_H = 4\times10^{-20}$ J) of foam films with 0.5 mM of the halide counterions. The maxima of $\Pi(h)$ around $h = 5$ nm control the stability and the coalescence of the bubbles. The maximum is more than 4 times lower in the presence of only 0.5 mM Br than it would have been with the same electrolyte concentration if the ion specific effects were disregarded.

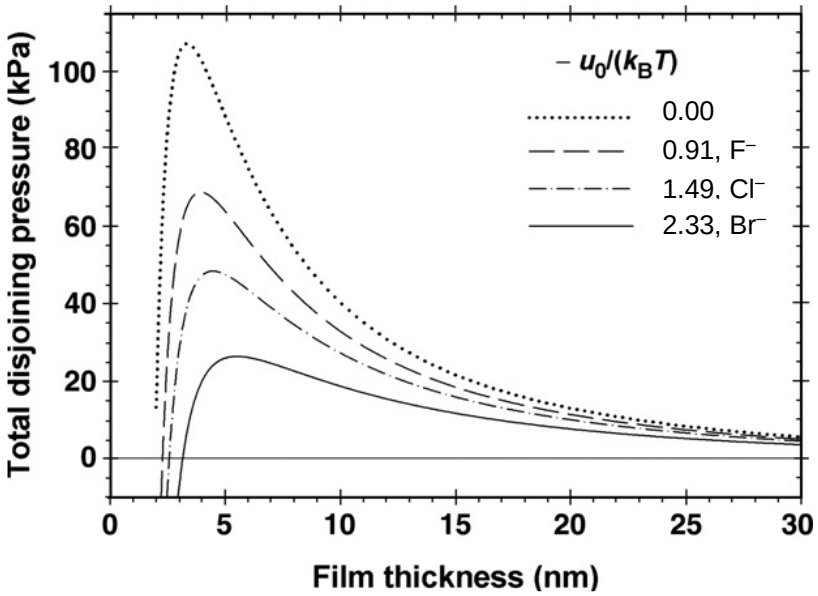

Figure 15. Total disjoining pressure Π_{total} calculated with Hamaker constant $A_H = 4\times10^{-20}$ J for 0.5 mM counter-ions F^-, Cl^- and Br^- (from Ref. [26]).

3.2. Ion-Specific Effects on the Stability of Dispersed Systems

3.2.1. Emulsion Stability

Ref. [27] reports on the emulsion stability measured by means of two types of techniques – Film Trapping Technique (FTT) and Centrifugation. They used the same surfactant ($C_{16}H_{33}NMe_3Br$) and salts (NaF, NaCl or NaBr). The concentrations of the surfactant and the added salts for FTT were the same as in the thin film studies described here above, but for the centrifugation the emulsions with 1 mM salts were too unstable, so that the concentrations of the added salts were increased to 30 mM. Soybean oil, purified by passing it through a glass column filled with Silicagel 60 adsorbent, was used as oil phase.

The film trapping technique (FTT), developed in Ref. [61-64] is a useful method for determining the coalescence stability of single emulsion drops. The principle of the FTT is the following: A vertical capillary, partially filled with oil, is held at a small distance above the flat bottom of a glass vessel, Figure 16. The lower edge of the capillary is immersed in the working solution, which contains dispersed micronsize oil drops. The capillary is connected to a pressure control system, which allows one to vary and to measure precisely the difference, ΔP_A, between the air pressure in the capillary, P_A, and the atmospheric pressure, P_A^0. The pressure is measured by a pressure transducer connected to a personal computer. Upon the increase of P_A the oil-water meniscus in the capillary moves downward against the substrate. When the distance between the oil-water meniscus and the glass substrate becomes smaller than the drop diameter, some of the drops remain entrapped in the formed glass-water-oil layer. The pressure P_A is increased until the coalescence of the entrapped oil drops with the upper oil phase is observed. The capillary pressure in the moment of drop coalescence, P_C^{CR}, represents the coalescence barrier and is called *critical capillary pressure*. It is related to ΔP_A in the moment of drop breakage and can be calculated from the equation:

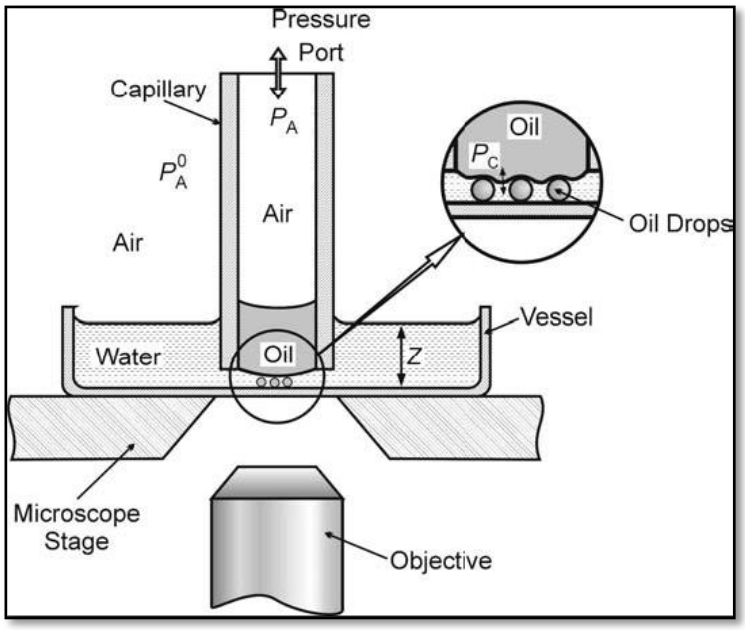

Figure 16. Scheme of the film trapping apparatus and of the droplets trapped between the oil-water and the substrate (see the magnification lens), from Ref. [64].

$$P_C^{CR} = \Delta P_A - \Delta P_{OIL} - \rho g z \quad (80)$$

Where, ΔP_{OIL} is the pressure jump across the oil column in the capillary. It includes contributions from the hydrostatic pressure of the oil column and the capillary pressure of the air|oil meniscus. It is measured after filling the FTT capillary with oil but before immersing the capillary into the water pool. In the hydrostatic term z is the depth of the water (Figure 16), ρ is the water mass density and g is gravity acceleration. The trapped oil drops and the coalescence process were observed from above with an optical microscope.

The test of the emulsion stability by means of centrifugation in described in details in Ref. [27]. Oil-in water emulsions were prepared by stirring for 4 min a mixture of 40 mL water phase and 10 mL soybean oil (20 vol. % SBO) with a rotor-stator homogenizer, Ultra Turrax T25 (Janke & Kunkel GmbH & Co, IKA-Labortechnik), operating at 13500 rpm. The drop size d_{32} was determined by optical microscopy of specimens of the studied emulsions in transmitted light with microscope. After 30 min storage the fresh emulsions were transferred into several centrifugal tubes and centrifuged at 25°C in 3K15 centrifuge. The emulsion stability is characterized by the critical osmotic pressure, P_{OSM}^{CR}, at which a continuous oil layer is released at the top of the emulsion cream in the centrifuge tube. P_{OSM}^{CR} is calculated from the experimental data by using the equation :

$$P_{OSM}^{CR} = \Delta\rho g_k \left(V^{OIL} - V^{REL}\right)/A = \Delta\rho g_k \left(H^{OIL} - H^{REL}\right) \quad (81)$$

Where $\Delta\rho$ is the difference between the mass densities of the aqueous and the oil phases; g_k is the centrifugal acceleration ($g_k = L\omega^2$, where L is the distance between the axis of rotation and the center of the cream, ω is the angular velocity); V_{OIL} is the total volume of oil used for preparation of the emulsion; V_{REL} is the volume of released oil at the end of centrifugation; and A is the cross-sectional area of the centrifuge test tube.

The results from both tests are presented in Table 4 and Figure 17.

Table 4. Critical pressures and drop sizes of SBO-in-water emulsions, stabilized with 1 mM $C_{16}H_{33}NMe_3Br$ with added NaF, NaCl and NaBr.

C_t [mM]	C_s [mM]	C_{el} [mM]	Electrolyte	d_{32} [μm]	FTT, P_C^{CR} [Pa]	Centrifuge, P_{OSM}^{CR} [Pa]
10	1	9	NaF	25.2	360	-
10	1	9	NaCl	28.5	1100	-
10	1	9	NaBr	27.0	1320	-
31	1	30	NaF	20.7	-	360
31	1	30	NaCl	22.4	-	640
31	1	30	NaBr	21.5	-	917

The systems parameters and the measured values of the critical pressures P_C^{CR} and P_{OSM}^{CR} are tabulated in Table 3 and plotted in Figure 17 as P_C^{CR} (solid line) and P_{OSM}^{CR} (dashed line) vs. $-u_0/k_BT$. These critical pressures are proportional to Π and the higher their values are, the more stable the emulsions.

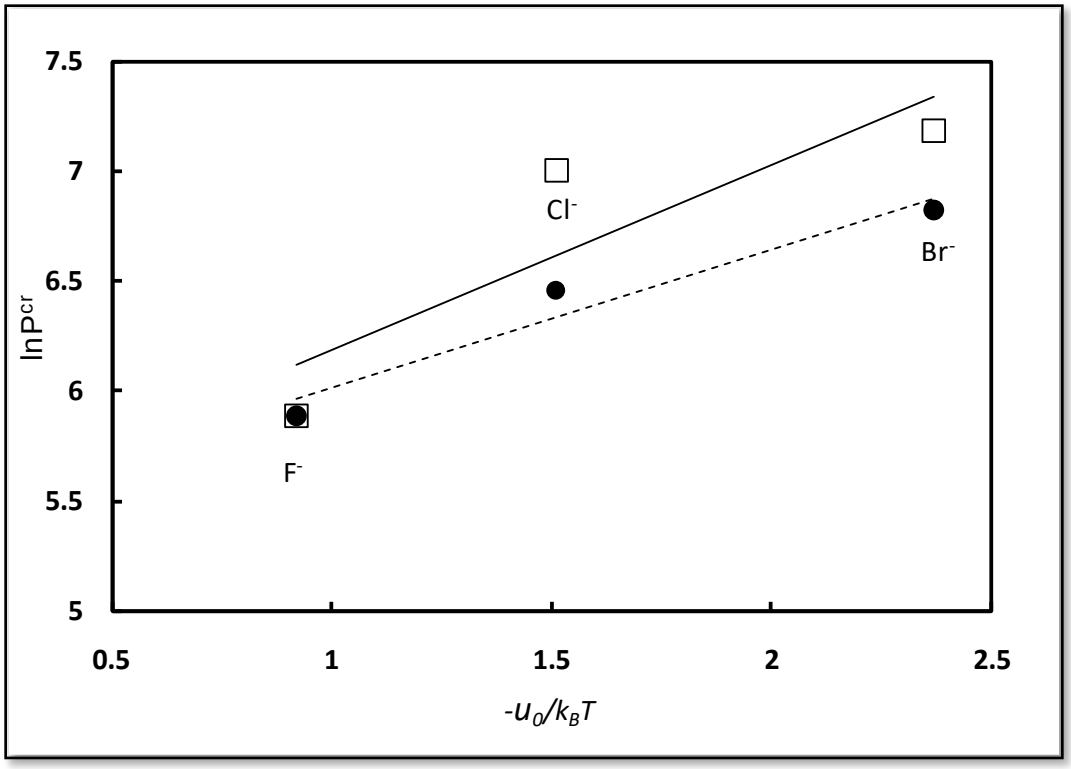

Figure 17. Critical pressures P_C^{CR} (by FTT, solid line) and P_{OSM}^{CR} (by centrifugation, dashed line) vs. $-u_0/k_BT$ of oil-in-water emulsions stabilized by $C_{16}H_{33}NMe_3Br$ + NaX (X=F^-, Cl^-, Br^-). (□) P_{OSM}^{CR} of oil-in-water emulsion films stabilized by 10^{-3} M $C_{16}H_{33}NMe_3Br$ + 9×10^{-3} M NaX (X=F^-, Cl^-, Br^-) obtained by FTT (slope = 0.85); (•) P_C^{CR} of oil-in-water emulsion films stabilized by 10^{-3} M $C_{16}H_{33}NMe_3Br$ + 3×10^{-2} M NaX (X=F^-, Cl^-, Br^-) obtained by centrifuge (slope=0.63).

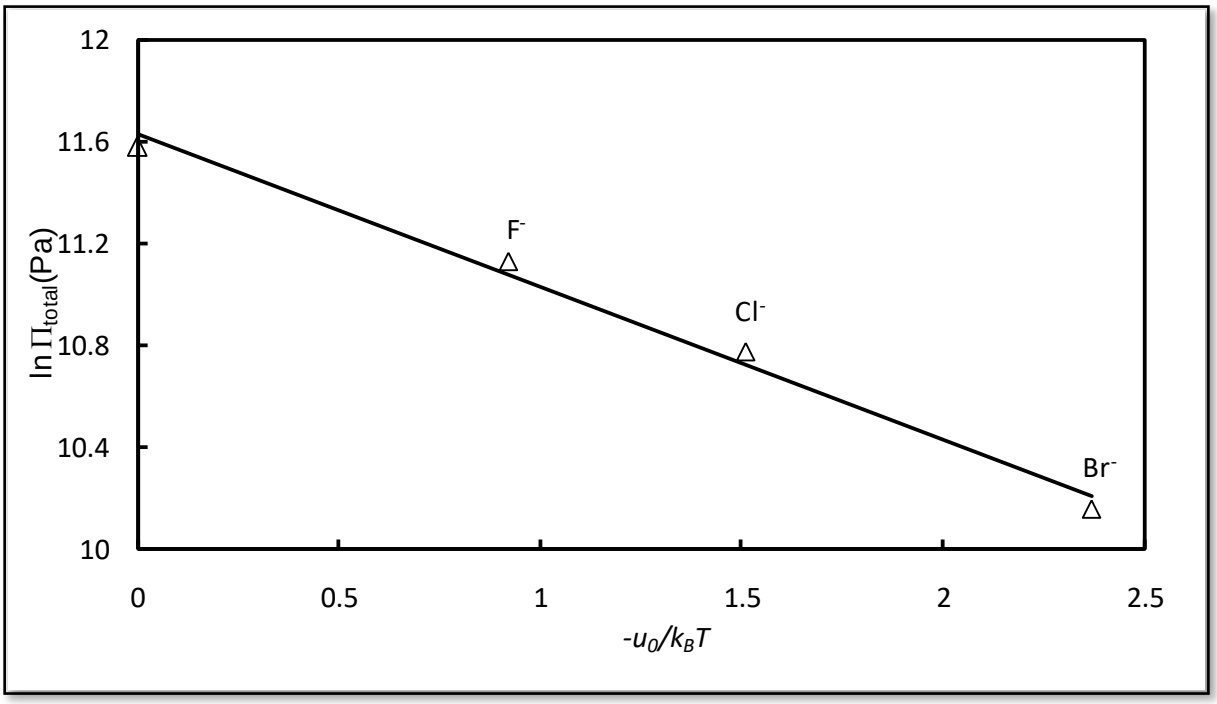

Figure 18. Total disjoining pressure Π_{total} in the maxima in Figure 13 vs. $-u_0/k_BT$. This is in fact the coalescence barrier, according to DLVO theory.

We do not dispose of enough information to carry out the same detailed analysis of these phenomena as we did with the electrostatic disjoining pressure. For example, we have no idea what the film thickness is; it is not quite clear whether a planar film forms or how much the disjoining pressure is affected by the curvature of the very small drops-these effects make problematic the calculation of the electrostatic disjoining pressure by means of Equation (77). Still, some qualitative conclusions are possible. The linear dependence of $P_{\mathrm{C}}^{\mathrm{CR}}$ and $P_{\mathrm{OSM}}^{\mathrm{CR}}$ on $-u_0/k_{\mathrm{B}}T$ confirms the presence of specific effects. However, instead of decreasing with the increase of $-u_0/k_{\mathrm{B}}T$ (as the electrostatic disjoining pressure does) the critical pressures are increasing. Therefore, the electrostatic disjoining pressure Π_{el} is not the repulsive pressure to be overcomed in order for the coalescence to occur. But then, what is the reason for the ion specific effect, demonstrated in Figure 18? It is not possible to answer with certitude this question without detailed studies of the phenomena accompanying the coalescence process. Nevertheless we dare suggesting a hypothesis. The role of the specific effect of the counterions is twofold. On one side, it decreases the height of the maxima of the disjoining pressure (see Figure 15) thus making easier for the thin film to avoid the electrostatic repulsive pressure and to thin to thinner (metastable) Newton black film, where another, short range repulsive disjoining pressure (most probably steric or osmotic) might be operative. It must be overcomed for the thin film to rupture. On the other side, no matter what the nature of this disjoining pressure is, it must increase with the surfactant adsorption, Γ. However, unlike the electrostatic disjoining pressure, the surfactant adsorption, Γ, increases (for a given bulk surfactant concentration) with $-u_0/k_{\mathrm{B}}T$ (cf. Equation (73)). This brings us to the second role of the ion specific effects – it is to increase the short range

repulsive pressure created by the surfactant, thus stabilizing the thin film. This explains why the slopes of the lines in Figure 13 are positive. They should have been negative if only the electrostatic disjoining pressure Π_{el} were stabilizing the film. To support this opinion in Fig. 18 we have plotted the maxima of Π_{total} from Fig. 15 (which are in fact the coalescence barriers) vs. $-u_0/k_BT$ –indeed, the slope is negative. This means that the short range repulsive pressure involved in the stability of the emulsion drops is not directly related to ion specific effects. The theoretical and experimental verification of this hypothesis is feasible, but it is time consuming and beyond the scope of this paper.

3.2.2. Foam Stability

We have established that the stability of the emulsions increases upon enhancing the specific adsorption energy of the counter-ions. This tendency was not expected.

For this reason, we were challenged to investigate this scientific "intrigue" deeper. We have chosen another system – foam stabilized by sodium dodecyl sulfate (SDS) and LiCl, NaCl and KCl as salts, which were meant to be added in amount significantly exceeding this one of the surfactant.

We clearly showed hereafter that the electrostatic repulsion between the bubbles, which is controlled by the added counter-ions, is only one of the factors contributing to foam stabilization. The counter-ions strongly affect the level of surfactant adsorption as well. The latter appear to be decisive for the stabilization of the foam and the foam films. We show as well some new effects originating from the counter-ions, which have practical significance.

Sodium dodecyl sulfate (SDS) with molecular weight M_w = 288.38 Da, an anionic surfactant, lithium chloride (LiCl) with molecular weight M_w = 42.29 Da, sodium chloride (NaCl) with molecular weight M_w = 58.44 Da, and potassium chloride (KCl) with molecular weight M_w = 74.55 Da were purchased from Sigma Aldrich. The surfactant was purified by threefold re-crystallization in ethanol.

SDS salt mixture solutions were prepared as follows. Initially, using SDS, 0.5 mM aqueous solution was prepared. Then, LiCl, NaCl and KCl, were added, thus forming salt solutions with concentrations in the range of 2.5 mM, to 50 mM. As far as the foaming ability of every surfactant solution is expressed in both the initial foam volume upon the very generation of foam and the lifetime of the latter, we chose to work with the ratio between the two values, called foam production [65]. The foam was produced by means of the Bartsch method expressed in energetical tenfold shaking of Bartsch column containing 50 ml of the surfactant solution. Each experiment was repeated at least 3 times for statistical certainty and the averaged initial foam volume and lifetimes were determined. Thus, the foam production for every particular case was calculated. The basic results are presented in Figure 19.

One can see that the foam production increases linearly upon the increase of the specific energy of counter-ions adsorption in the range of 2.5 mM to 11 mM added salt (Figure 19A). Moreover, this linear dependence is violated by K^+ counter-ion at concentrations of added salt above 11 mM (see Figure 19B, 19C, 19D). The foam production decreases significantly abruptly at 25 mM KCl. This low value of the foam production remains at a larger concentration of KCl. They correspond to both low initial foam volume and fast foam decay.

This abnormal effect of KCl on the foam production is worthy of further investigation. Possible way for such an investigation to explore the properties of single foam films with the same contents as these ones in Figure 19. Moreover, it is curious to know if the critical concentration at which the K^+ ion acts as de-foamer depends on the method of foam generation.

The experimental data presented in Figure 19A are in line with the experimental data reported in Ref. [27]. The the stability of the dispersed system increases upon the increase of the absolute value of the specific adsorption energy of the counter-ions on the air| water interface. Most possibly this is due to the increased level of the surfactant adsorption when more counter-ions are integrated in the surfactant adsorption layer. However, to investigate this effect on deeper level further investigations are needed.

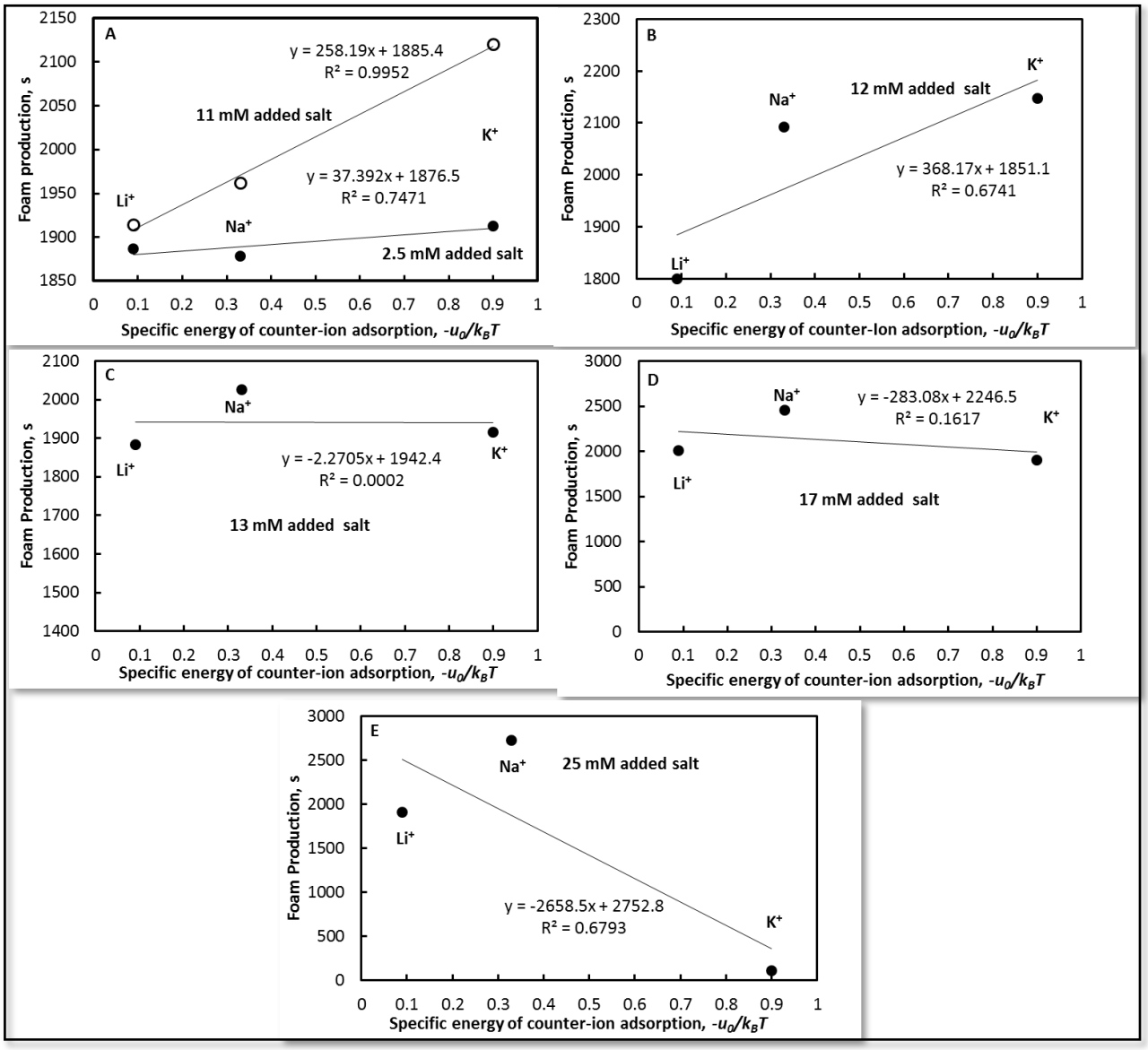

Figure 19. Foam production versus specific energy of counter-ion adsorption at concentrations of added salt in the range of 2.5 mM – 25 mM.

4. Conclusions

The ion-specific effects on the adsorption of ionic surfactants are known effect. There is a large body of literature on this topic, but it is spread out in many papers and books at present. It is known as well that the counter-ions affect the state of the adsorbed layers, which influences the stability of the colloidal dispersions, but the effect is not studied completely. This manuscript gathers together detailed description of theory on the ion-specific effects on the adsorption of ionic surfactants in its present state and some initial experimental studies of the Hofmeister effect on the stability of foams and emulsions.

4. Conflicts of Interest

The author(s) report(s) no conflict(s) of interest(s). The author along are responsible for content and writing of the paper.

5. Acknowledgement

This work was supported by DT/IA Resource Centre, Ton Duc Thang University, Ho Chi Minh City, Vietnam.

6. References

1. Lewith S. To the theory of the effect of the salts. Archive for Experimental Pathaology and Pharmacology 1887; 24(1-2): 1-16.
2. Hofmeister F. To the theory of the effect of the salts (Second message). Archive for Experimental Pathaology and Pharmacology 1888; 24(4-5): 247-260.
3. Hofmeister F. To the theory of the effect of the salts (First message). Archive for Experimental Pathaology and Pharmacology 1888; 25(1): 1-30.
4. Limbeck RV. To the theory of the effect of the salts (On the Diuretic Effect of Salts). Archive for Experimental Pathaology and Pharmacology 1888; 25(1): 69-86.
5. Hofmeister F. To the theory of the effect of the salts (Free and disabled swelling). Archive for Experimental Pathaology and Pharmacology 1890; 27(6): 395-413.
6. Hofmeister F. To the theory of the effect of the salts (The participation of dissolved substances in swelling processes). Archive for Experimental Pathaology and Pharmacology 1891; 28(3-4): 210-238.
7. Muenzer E. To the theory of the effect of the salts (The general effect of salts). Archive for Experimental Pathaology and Pharmacology 1898; 41(1): 74-96.
8. Kunz W, Nostro PL, Ninham BW. The present state of affairs with Hofmeister effects. Current Opinion in Colloid and Interface Science 2004; 9(1): 1-18.
9. Ninham BW. On progress in forces since the DLVO theory. Advances in Colloid & Interface Science 1999; 83(1-3): 1-17.
10. Ninham BW, Yaminsky V. Ion binding and ion specificity: The Hofmeister effect and Onsager and Lifshitz theories. Langmuir 1997; 13(7): 2097-2108.
11. Bostrom M, Williams DRM, Ninham BW. Specific ion effects: Why DLVO theory fails for biology and colloid systems. Physical Review Letters 2001; 87(16): 168103.
12. Bostroem M, Williams DRM, Ninham BW. Surface tension of electrolytes: Specific ion effects explained by dispersion forces. Langmuir 2001; 17(15): 4475-4478.

13. Bostrom M, Kunz W, Ninham BW. Hofmeister effects in surface tension of aqueous electrolyte solution. Langmuir 2005; 21(6): 2619-2623.
14. Moreira LA, Bostrom M, Ninham BW, Biscaia EC, Tavares FW. Hofmeister effects: Why protein charge, pH titration and protein precipitation depend on the choice of background salt solution. Colloids and Surfaces A: Physicochemical and Engineering Aspects 2006; 282-283: 457-463.
15. Bostroem M, Ninham BW. Contributions from dispersion and born self-free energies to the solvation energies of salt solutions. The Journal of Physical Chemistry B 2004; 108(33): 12593-12595.
16. Tavares FW, Bratko D, Blanch HW, Prausnitz JM. Ion-specific effects in the colloid-colloid or protein-protein potential of mean force: Role of salt-macroion van der Waals interactions. The Journal of Physical Chemistry B 2004; 108(26): 9228-9235.
17. Warszynski P, Lunkenheimer K, Czichocki G. Effect of counterions on the adsorption of ionic surfactants at fluid-fluid interfaces. Langmuir 2002; 18(7): 2506-2514.
18. Para G, Jarek E, Warszynski P. The Hofmeister series effect in adsorption of cationic surfactants - theoretical description and experimental results. Advances in Colloid & Interface Science 2006; 122(1-3): 39-55.
19. Para G, Jarek E, Warszynski P. The surface tension of aqueous solutions of cetyltrimethylammonium cationic surfactants in presence of bromide and chloride counterions. Colloids and Surfaces A: Physicochemical and Engineering Aspects 2005; 261(1-3): 65-73.
20. Li HH, Imai Y, Yamanaka M, Hayami Y, Takiue T, Matsubara H, Aratono M. Specific counterion effect on the adsorbed film of cationic surfactant mixtures at the air/water interface. Journal of Colloid and Interface Science 2011; 359(1): 189-193.
21. Shimamoto K, Onohara A, Takumi H, Watanabe I, Tanida H, Matsubara H, Takiue T, Aratono M. Miscibility and distribution of counterions of imidazolium ionic liquid mixtures at the air/water surface. Langmuir 2009; 25(17): 9954-9959.
22. Hayami Y, Ichikawa H, Someya A, Aratono M, Motomura K. Thermodynamic study on the adsorption and micelle formation of long chain alkyltrimethylammonium chlorides. Colloid and Polymer Science 1998; 276(7): 595-600.
23. Davies JT. Adsorption of long-chain ions. I. Proceedings of Royal Society A: Mathematical, Physical and Engineering Science 1958; 245(1242): 417-428.
24. Davies JT, Rideal EK. Interfacial phenomena. 2nd edition, Academic Press, USA, 1963.
25. Borwankar RP, Wasan DT. Equilibrium and dynamics of adsorption of surfactants at fluid-fluid interfaces. Chemical Engineering Science 1988 43(6): 1323-1337.
26. Ivanov IB, Marinova KG, Danov KD, Dimitrova D, Ananthapadmanabhan KP, Lips A. Role of the counterions on the adsorption of ionic surfactants. Advances in Colloid and Interface Science 2007; 134-135: 105-124.
27. Ivanov IB, Slavchov RI, Basheva ES, Sidzhakova D, Karakashev SI. Hofmeister effect on micellization, thin films and emulsion stability. Advances in Colloid and Interface Science 2011; 168(1-2): 93-104.

28. Ivanov IB, Ananthapadmanabhan KP, Lips A. Adsorption and structure of the adsorbed layer of ionic surfactants. Advances in Colloid and Interface Science 2006; 123-126: 189-212.
29. Slavchov RI, Karakashev SI, Ivanov IB. Ionic surfactants and ion-specific effects: Adsorption, micellization, thin liquid films. In: Romsted LS (Ed). Surfactant science and technology: Retrospects and prospects. Taylor & Francis Group, 2014, pp. 593.
30. Tanford C. The hydrophobic effect. Wiley, USA, 1980.
31. Karakashev SI. How to determine the adsorption energy of the surfactant's hydrophilic head? How to estimate easily the surface activity of every simple surfactant? Journal of Colloid and Interface Science 2014; 432: 98-104.
32. Gibbs JW. The collected works, Longmans, 1928.
33. Robinson RA, Stokes RH. Electrolyte Solutions. 2nd edition, Butterworth & Co., USA, 1959.
34. Lucassen-Reynders EH. Surface equation of state for ionized surfactants. The Journal of Physical Chemistry 1966; 70(6): 1777-1785.
35. Davies JT. Study of foam stabilizers using a new (\"viscous-traction\") surface viscometer. Proceedings: International Congress of Surface Activity (2nd), London, 1957, pp. 220-224.
36. Langmuir I. Theory of adsorption. Physical Review 1915; 6: 79-80.
37. Aratono M, Uryu S, Hayami Y, Motomura K, Matuura R. Phase-transition in the adsorbed films at water air interface. Journal of Colloid and Interface Science 1984; 98(1): 33-38.
38. Gurkov TD, Dimitrova DT, Marinova KG, Bilke-Crause C, Gerber C, Ivanov IB. Ionic surfactants on fluid interfaces: determination of the adsorption; role of the salt and the type of the hydrophobic phase. Colloids and Surfaces A: Physicochemical and Engineering Aspects 2005; 261(1-3): 29-38.
39. Rehfeld SJ. Adsorption of Sodium Dodecyl Sulfate at Various Hydrocarbon-Water Interfaces. The Journal of Physical Chemistry 1967; 71(3): 738-745.
40. Hines JD. The preparation of surface chemically pure sodium n-dodecyl sulfate by foam fractionation. Journal of Colloid and Interface Science 1996; 180(2): 488-492.
41. Haydon DA, Taylor FH. On adsorption at the oil-water interface and the calculation of electrical potentials in the aqueous surface phase .1. Neutral molecules and a simplified treatment for ions. Philosophical Transactions of the Royal Society of the London. Series A, Mathematical and Physical Sciences 1960; 252(1009): 225-248.
42. Israelachvili JN. Intermolecular and surface forces. Academic Press, USA, 1985.
43. Izmailov NA. Electrochemistry of solutions. 3rd edition, Khimia, 1976.
44. Marcus Y. Ion properties. Marcel Dekker, USA, 1997.
45. Marcus Y. Thermodynamics of ion hydration and its interpretation in terms of a common model. Pure and Applied Chemistry 1987; 59(9): 1093-1101.
46. Kunz W, Belloni L, Bernard O, Ninham BW. Osmotic coefficients and surface tensions of aqueous electrolyte solutions: Role of dispersion forces. The Journal of Physical Chemistry B 2004; 108(7): 2398-2404.
47. Nikolskij BP. Handbook of the chemist (In Russian), Khimia, 1966.

48. Dietrich B, Kintzinger JP, Lehn JM, Metz B, Zahidi A. Stability, molecular-dynamics in solution, and X-Ray structure of the Ammonium Cryptate [Nh4+-Subset-of-2.2.2]Pf6. The Journal of Physical Chemistry 1987; 91(27): 6600-6606.
49. Lide DR. Handbook of chemistry and physics. 83rd edition, CRC Press, USA, 2002.
50. Gillap WR, Weiner ND, Gibaldi M. Effect of hydrocarbon chain length on adsorption of sodium alkyl sulfates at oil/water inter. Journal of Colloid and Interface Science 1968; 26(2): 232-236.
51. Aveyard R, Briscoe BJ. Adsorption of n-alkanols at alkane/water interfaces. Journal of the Chemical Society, Faraday Transactions 1: Physicl Chemistry in Condensed Phases 1972; 68(0): 478-491.
52. Haydon DA, Taylor FH. Adsorption of sodium octyl and decyl sulphates and octyl and decyl trimethylammonium bromides at the decane-water interface. Transactions of the Faraday Society 1962; 58: 1233-1250.
53. Bergeron V. Disjoining pressures and film stability of alkyltrimethylammonium bromide foam films. Langmuir 1997; 13(13): 3474-3482.
54. Das C, Das B. Effect of tetraalkylammonium salts on the micellar behavior of lithium dodecyl sulfate: A conductometric and tensiometric study. Journal of Molecular Liquids 2008; 137(1-3): 152-158.
55. Lu JR, Marrocco A, Su T, Thomas RK, Penfold J. Adsorption of dodecyl sulfate surfactants with monovalent metal counterions at the air-water interface studied by neutron reflection and surface tension. Journal of Colloid and Interface Science 1993 158(2): 303-316.
56. Koelsch P, Motschmann H. Varying the counterions at a charged interface. Langmuir 2005; 21(8): 3436-3442.
57. Rogers J, Schulman JH. Proceedings of Second International Congress of Surface Activity. In: Schulman JH (Ed). Intern congr surface activity. Butterworth, London, 1957, pp. 243.
58. Sears DF, Schulman JH. Influence of water structures on the surface pressure, surface potential, and area of soap monolayers of Lithium, Sodium, Potassium, and Calcium. The Journal of Physical Chemistry 1964; 68(12): 3529-3534.
59. Weil I. Surface concentration and the Gibbs adsorption law. The effect of the alkali metal cations on surface behavior. The Journal of Physical Chemistry 1969; 70(1): 133-140.
60. Churaev NV, Derjagiun BV, Muller VM. Surface Forces. Springer, Germany, 1987.
61. Ivanov IB, Hadjiiski A, Denkov ND, Gurkov TD, Kralchevsky PA, Koyasu S. Energy of adhesion of human T cells to adsorption layers of monoclonal antibodies measured by a film trapping technique. Biophysical Journal 1998; 75(1): 545-556.
62. Hadjiiski A, Dimova R, Denkov ND, Ivanov IB, Borwankar R. Film trapping technique - Precise method for three-phase contact angle determination of solid and fluid particles of micrometer size. Langmuir 1996; 12(26): 6665-6675.
63. Hadjiiski A, Tcholakova S, Ivanov IB, Gurkov TD, Leonard EF. Gentle film trapping technique with application to drop entry measurements. Langmuir 2002; 18(1): 127-138.

64. Tcholakova S, Denkov ND, Ivanov IB, Campbell B. Coalescence in beta-lactoglobulin-stabilized emulsions: Effects of protein adsorption and drop size. Langmuir 2002; 18(23): 8960-8971.
65. Karakashev SI, Georgiev P, Balashev K. Foam production ratio between foaminess and rate of foam decay. Journal of Colloid and Interface Science 2012; 379(1): 144-147.